

Kristine Eide

Synthesis of Covalently Functionalized Graphene Hybrids for Use in Carbon Capture Membranes

Functionalization of graphene with 2-(2-(2-ethoxyethoxy)ethoxy)ethylmalonate

Master's thesis in MLREAL

Supervisor: Solon Oikonomopoulos

June 2020

Kristine Eide

Synthesis of Covalently Functionalized Graphene Hybrids for Use in Carbon Capture Membranes

Functionalization of graphene with 2-(2-(2-ethoxyethoxy)ethoxy)ethylmalonate

Master's thesis in MLREAL
Supervisor: Solon Oikonomopoulos
June 2020

Norwegian University of Science and Technology
Faculty of Natural Sciences
Department of Chemistry



PREFACE

This master thesis is written under the study program “Lektorutdanning i Realfag” (MLREAL) at Norwegian University of Science and Technology (NTNU) from January to June 2020. Working on this master have given me valuable insight in the field of research in chemistry and my curiosity have been increased. As a teacher I believe and hope that my interest and eagerness for chemistry can inspire the students.

I would like to thank my supervisor Solon Oikonomopoulos for all his guidance, and for his good mood through the whole process. A big thanks to Roger Aarvik for always supplying everything I need of both chemicals and glassware. Thanks to Torun Melø for training in NMR – analysis, and Julie Asmussen/Susana Gonzales for running MS-samples. I would also like to thank everyone in lab D2-199 for assistance, good advices, and for a good atmosphere. Thanks to Sigmund for help with Raman analyses and answering a lot of questions.

Last, but not least, I would like to thank my fellow students and good friends, Kristine, Eirik and Natalie, for good corporation through all these years and for all the breaks with card games and conversations about everything and nothing. You have made this a whole lot more fun.

Abstract

Abstract

Due to the large emission of CO₂, the world is facing environmental challenges. Carbon Capture and Storage (CCS) technology can reduce the amount of CO₂ in the atmosphere and research in this field is of great importance. In this project graphene hybrids were made by covalent attachment of 2-(2-(2-ethoxyethoxy)ethoxy)ethylethylmalonate onto graphene for use in Mixed Matrix Membranes (MMM) in CCS. Graphene was made by sonication of graphite in NMP using tip sonication at 63 W. 2-(2-(2-Ethoxyethoxy)ethoxy)ethylethylmalonate was made through an esterification reaction of 2-(2-(2-ethoxyethoxy)ethoxy)ethane-1-ol and ethyl-3-chloro-3-oxopropanoate going through a nucleophilic acyl substitution. The covalent attachment of the malonate was done through a microwave assisted Bingel reaction and Raman spectroscopy and the colour of the samples indicated that functionalization had taken place.

Using 0,01 mL of malonate, about 0,07 g CBr₄ and 0,05 mL of DBU for 3 mL of graphene with a reaction time of 10 minutes in the microwave seemed to be the most efficient way of functionalizing graphene with the malonate.

Samandrag

Samandrag

For å få bukt med miljøutfordringane som verda står ovanfor i dag kan karbonfangst og lagrings – teknologien (CCS) bli svært viktig for å kunne redusere mengda CO₂ i atmosfæren. I dette prosjektet vert det produsert grafen hybridar ved å kovalent funksjonalisere grafen med 2-(2-(2-etoksyetoksy)etoksy)etyletylmalonat for å bruke i «Mixed Matrix Membranes» (MMM) i CCS. Grafen vart produsert ved å sonikere grafitt i NMP ved bruk av «tip-sonication» på 63 W. 2-(2-(2-Etoksyetoksy)etoksy)etyletylmalonat vart syntetisert gjennom ein esterifiserings reaksjon av 2- (2- (2-etoksyetoksy)etoksy)etan-1-ol og etyl-3-klor-3-oksopropanoat via ein nukleofil asylsubstitusjon. Kovalent funksjonalisering av grafen med malonaten vart utført gjennom ein mikrobølge-assistert Bingel reaksjon. Raman spektroskopi og fargen på prøvene indikerte at funksjonalisering hadde skjedd. Optimalisering av funksjonaliseringsreaksjonen blei gjort og det som verka å vere den mest effektive måten var å bruke 0,01 ml malonat, rundt 0,07 g CBr₄ og 0,05 ml DBU for 3 ml grafen med ei reaksjonstid på 10 minutt når mikrobølgjer vert nytta.

Abbreviations

<i>o</i> -DCB	1,2-dichlorobenzene
DCM	Dichloromethane
NMP	<i>N</i> -methyl-2-pyrrolidinone
DBU	1,8-Diazabicyclo(5.4.0)undec-7-ene
EO	Ethylene oxide
PEG	Polyethylenoglycol
GO	Graphene oxide
CCS	Carbon Capture and Storage
RFG	Recycled flue gas
MMM	Mixed matrix membrane
CNH	Carbon nano horn
SWNT	Single walled carbon nano tubes
DMF	Dimethylformamide
IR	Infrared
NMR	Nuclear Magnetic Resonance spectroscopy
MS	Mass Spectrometry
TGA	Thermogravimetric analysis
NETL	National Energy Technology Laboratory
IPCC	Intergovernmental Panel on Climate Change
PEI	Polyethylene imine
CVD	Chemical Vapor Deposition
PECVD	Plasma Enhanced Chemical Vapor Deposition
RGO	Reduced graphene oxide
LPE	Liquid phase exfoliation
GBL	Gamma-butyrolactone
HPC	Hydroxypropyl cellulose
TLC	Thin layer chromatography

Table of content

Abstract	III
Samandrag	IV
Abbreviations	V
1. Introduction	1
1.1 Carbon Capture and Storage.....	1
1.1.1 Pre combustion.....	3
1.1.2 Post combustion	3
1.1.3 Oxy-fuel combustion.....	4
1.2 Membranes in CCS	4
1.2.1 Mixed Matrix Membranes.....	6
1.3 Graphene	7
1.3.1 Graphene in CCS.....	7
1.3.2 Functionalization of graphene	8
1.3.3 Graphene oxide and graphene in mixed matrix membranes	9
1.4 Organic chemistry and synthesis	12
1.4.1 Synthesis of graphene.....	13
1.4.2 Chemistry on graphene.....	16
1.4.3 Synthesis of malonate.....	21
1.4.4 Microwave-assisted chemistry	23
Aim of the thesis	24
2. Results and discussion.....	25
3. Conclusion.....	41
Acknowledgements	41
4. Future work	42
5. Experimental	43
5.1 Preparation of 2-(2-(2-ethoxyetoxy)ethoxy)ethylethylmalonate.....	43
5.2 Preparation of graphene.....	44
5.3 Functionalization of graphene with 2-(2-(2-ethoxyetoxy)ethoxy)ethylethylmalonate.....	44
5.4 Workup of functionalized graphene	44
FAILED REACTIONS	45
5.5 Functionalization of graphene with 4-(2-aminoethyl)aniline.....	45
5.6 Characterization techniques	45
5.6.1 Infrared spectroscopy	45
5.6.2 Nuclear magnetic resonance spectroscopy	46
5.6.3 Raman spectroscopy.....	48

Table of content

5.6.4 Mass spectrometry	50
5.7 Solubility testing	50
7. References	51
8. Appendix	i
8.1 NMR – spectra of 2-(2-(2-ethoxyethoxy)ethoxy)ethylmalonate	i
8.2 MS of 2-(2-(2-ethoxyethoxy)ethoxy)ethylmalonate	vii
8.3 IR – spectra of 2-(2-(2-ethoxyethoxy)ethoxy)ethylmalonate	viii
8.4 Preparation and functionalization of graphene	ix
8.5 IR – spectra of functionalized graphene	xii

1. Introduction

In this chapter the relevant theory behind this project will be presented. An introduction on CO₂ in the atmosphere and the challenges the world is facing due to this, will be followed by theory about Carbon Capture and Storage (CCS) and the different capturing processes. Membranes as a separation technique will be presented followed by a section on graphene and how it can be used in membranes for CCS. In the end some organic synthesis will be presented.

From august 2018 to august 2019 the concentration of CO₂, the predominant greenhouse gas ¹, in the atmosphere increased from 406,91 ppm to 409,95 ppm (USDC, 2019) ². In 2009 the coal fired powerplants all over the world emitted around 2 billion tons of CO₂ ³. This leads to several environmental challenges such as global warming and climate changes ⁴, which are some of the greatest threats to human and animal health as well as political stability ⁵. To overcome these challenges, the emission of CO₂ and other greenhouse gases to the atmosphere, needs to be reduced. While an actual number is difficult to propose, according to studies, a reduction in today's emission of greenhouse gases by 80 % might be required towards global temperature stabilization ⁶.

In a developing world where the energy demand is ever rising, the emission of CO₂ will keep rising. It is essential to find efficient ways to produce energy which don't cause emission of CO₂. Today there are a lot of promising technologies like solar cells, hydropower plants and windmills. Although some these technologies are already commercially available or nearing mass-production, the existing infrastructure our society is based on, needs to be massively improved towards CO₂ emissions, while the transitioning period towards green energy sources occur. This is where the Carbon Capture and Storage (CCS) can come in handy. In the following section theory about CCS will be presented.

1.1 Carbon Capture and Storage

Bains *et. al* (2017) looks at Carbon Capture and Storage (CCS) as a bridge between today's fossil fuels and the future renewable energy ⁷. D'Alessandro *et. al* (2010) suggests CCS as a compliment to switching to less carbon-intensive fuels and phasing the use of renewable energy sources and sees CCS as a short to medium – term opportunity to meet the increasing demands for fossil fuel energy. IPCC estimates that a modern conventional powerplant can reduce the emission of CO₂ by 80 – 90 % if it is equipped with CCS technology ^{1, 8}. The challenge is that CCS – technology is energy intensive and yet not cost effective ⁸.

Introduction

The CCS process refers to removal of CO₂ directly from the sources before the CO₂ is compressed and transported to a storage, as shown in Figure 1.1.1¹. The CO₂ is deposited underground and it is important that the storage doesn't allow the CO₂ to be released back to the atmosphere⁹.

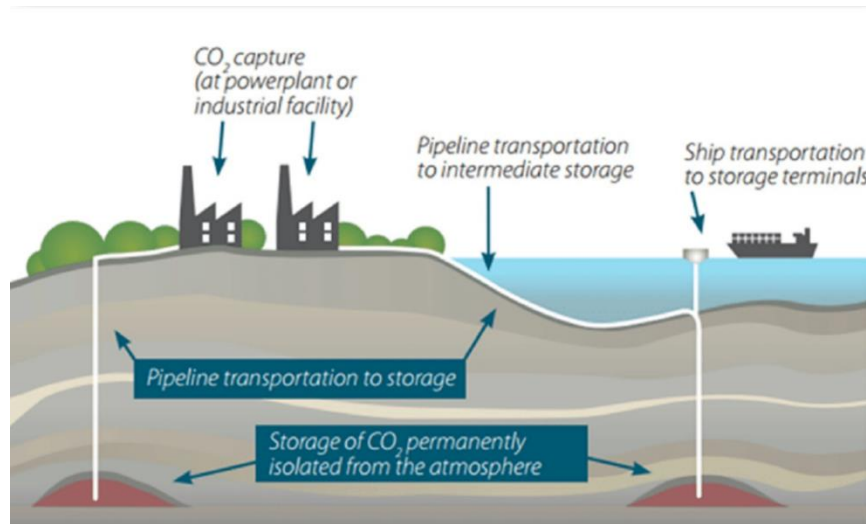


Figure 1.1.1: Principle of carbon capture and storage¹⁰.

Mainly there are three different processes used for CO₂ capture. They are referred to as pre-combustion, post-combustion and oxy-fuel combustion and they share many of the same separation techniques, as shown in Figure 1.1.2¹. In the following sections these three processes will be presented. The different separation techniques these processes are based on absorption, adsorption, cryogenic distillation, membranes, gas hydrates and chemical looping¹.

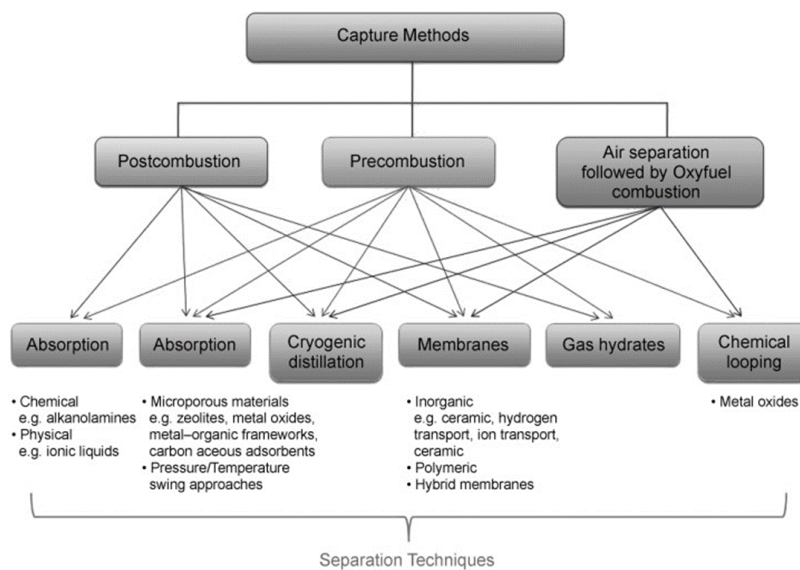


Figure 1.1.2: Capturing methods and separation techniques in CO₂ capture¹.

Introduction

1.1.1 Pre combustion

The first process is referred to as pre combustion since the CO₂ is separated and captured before the power generation (Fig 1.1.3). First the fossil fuel is gasified with stoichiometric amount of oxygen at elevated pressure and a syngas (that mainly consists of CO and H₂) is produced. The syngas goes through a water-shift reaction and CO is converted to CO₂ by addition of steam and decreasing the temperature. The CO₂ is then separated from H₂, and H₂ is used as an input in a combined cycle to produce energy ¹¹.

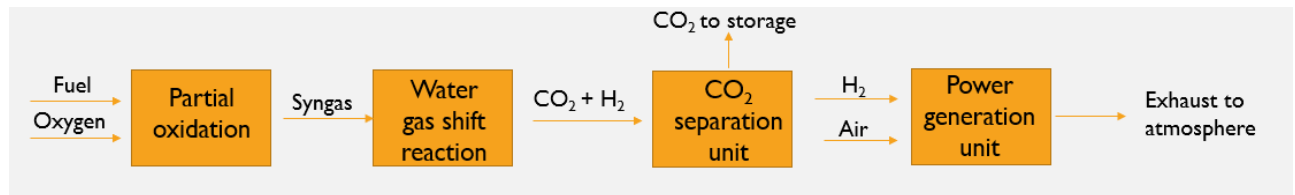


Figure 1.1.3: Pre-combustion process for CO₂ capture (figure inspired by Mondal *et al.* ¹¹).

There are several options for separation of the CO₂ gas, as shown in Figure 1.1.2. Absorption with a physical solvent is commonly used, where CO₂ is dissolved at high pressure and released as the pressure is reduced ¹¹. These physical solvents are often available at low costs and require low energy for regeneration. Pre-combustion capture can require half the energy compared to post-combustion. The disadvantage of pre-combustion capture is that it requires a chemical plant in front of the power generating turbine. This normally causes extra shutdowns which will cause a lower energy output. In addition the production of energy uses H₂ as an input, so it will not be possible to use this separation process on already existing power plants ¹¹.

1.1.2 Post combustion

Unlike pre-combustion the post-combustion capturing process can be used in already existing power plants by adding a separation unit at the end of the process. In post-combustion CO₂ is separated and captured from the flue gas that comes from the combustion, as shown in Figure 1.1.4. The fact that the separation process is not involved in the production of energy gives the conversion to electricity a higher thermal efficiency.

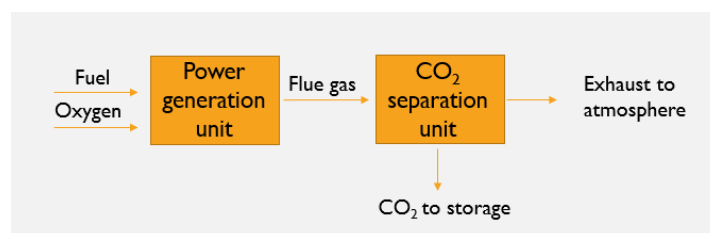


Figure 1.1.4: Post-combustion process for CO₂ capture (figure inspired by Mondal *et al.* ¹¹).

Typically the concentration of CO₂ in the flue gas is less than 15 % in existing power plants and this leads to some challenges. Since the concentration is low, the amount of flue gas needs to be large. This creates several technical challenges for development of cost-effective capturing processes and it also requires large equipment sizes which again leads to high capital costs. The temperature of the flue gas is normally high, and powerful solvents are needed. Releasing CO₂ from the solvent then requires a large amount of energy ¹¹.

1.1.3 Oxy-fuel combustion

The third process is referred to as the oxy-fuel combustion process. In this process the fuel is burned in a combustion chamber alongside pure O₂ and recycled flue gas (RFG) as shown in Figure 1.1.5. RGF is used because coal combustion in pure oxygen will generate such high temperatures that there are no currently available materials of construction that will be able to withstand at such high temperatures.

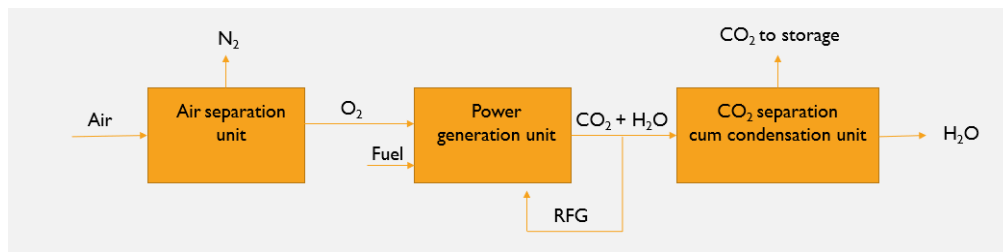


Figure 1.1.5: Oxy-fuel combustion process for CO₂ capture (figure inspired by Mondal *et al.* ¹¹).

After the combustion in O₂ the flue gas mainly consists of CO₂ and water vapor. The water can easily be removed by condensation and remaining CO₂ can be purified at relatively low costs ^{3, 11}. The economic benefit is reduced by the air separation needed to separate pure oxygen and by the recycling of the flue gas ¹¹.

1.2 Membranes in CCS

As shown in Figure 1.1.2 there are several capturing techniques used for carbon capture. This project will focus on the use of membranes as a separation technique in post combustion. Membranes is one of the latest concepts in carbon capture used to separate certain components from a gas stream (Fig 1.2.1), ¹¹ and allows a simple and efficient gas separation compared to other separation techniques ¹². The advantages of membranes in gas separation will be presented later in this section.

In post combustion, CO₂ is to be separated from the flue gas, in pre combustion, CO₂ is separated from hydrogen-gas and in oxy-fuel combustion, oxygen needs to be separated from nitrogen gas ¹¹. Membranes are semi-permeable and separates substances in various

Introduction

mechanisms. In a gas separation membrane, showed in Figure 1.2.1, the selectivity of the membrane and the permeability of the substances causes some components to diffuse through the membrane faster than others ¹¹. The different mechanisms that the separation can be achieved is solution/diffusion (Fig 1.2.2i), adsorption/diffusion (Fig 1.2.2ii), molecular sieve (Fig 1.2.2iii) or ionic transport (Fig 1.2.2iv) ¹¹.

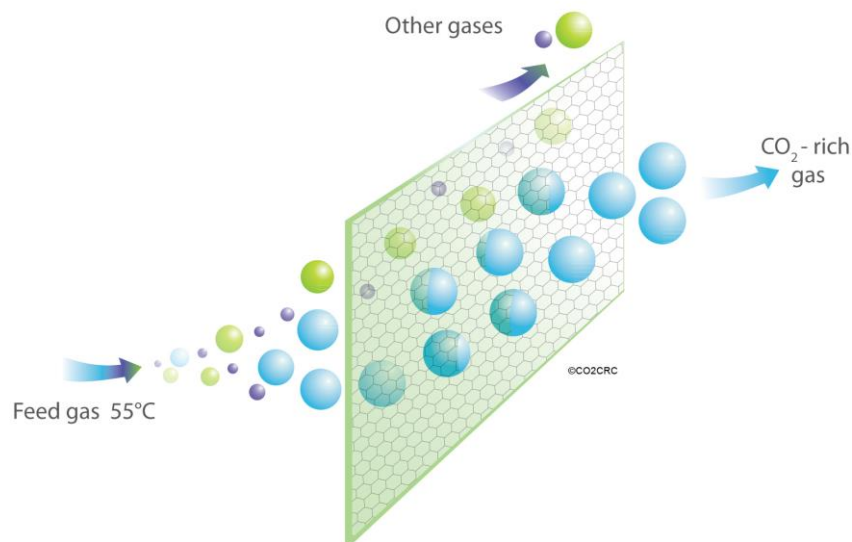


Figure 1.2.1: Membrane technology in CO₂ capture ¹³.

Membranes are responsible for separating substances and this can be done in several ways. One is size sieving (Fig 1.2.2iii) where the molecules are separated based on their size and the size of the pores in the membrane. In post combustion CO₂ are to be separated from N₂ and the difference in kinetic diameter is only 0.3 Å. To facilitate the separation, chemical functionalization of the membrane can be pursued. The functional groups must enhance the selective adsorption from the gas phase to the pores, and for separation of CO₂ functionalization with CO₂ – philic groups will be suited ¹³.

Introduction

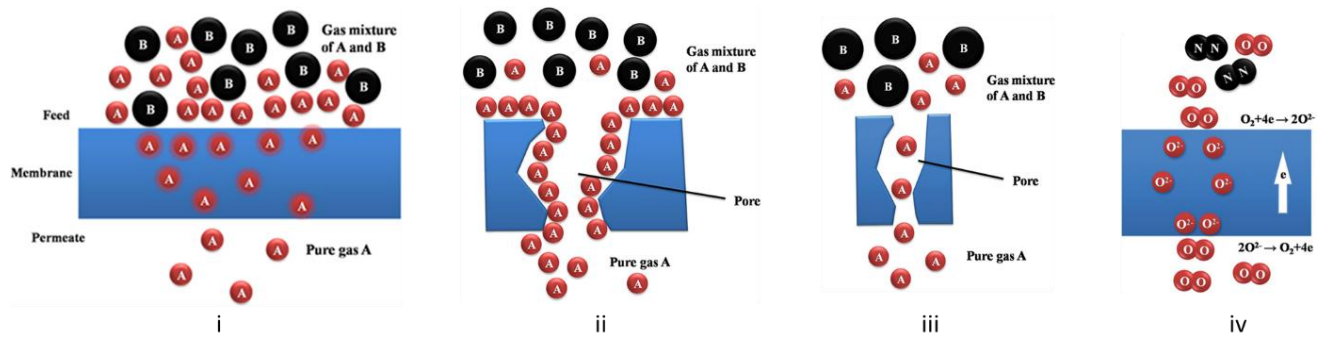


Figure 1.2.2: Schematic representation of i) Solution diffusion separation mechanism, ii) Surface diffusion separation mechanism iii) Size sieving separation mechanism and iv) Ion transport separation mechanism¹³.

The membrane technology is quite novel and the research on the field is continually growing due to the numerous advantages over competing separation technologies. Membranes have a low capital cost, and they don't require additional facilities. At the same time, the operating costs are low because there is no solvent or sorbent needed to be replaced. Membranes can run for a long time without supervision because they don't show a fast decay in performance. The membranes can be designed and operated to remove the required percentage of a gas, which makes it easy to adapt to the targeted process. Membranes are also said to be design efficient because a number of processes can be integrated in one unit. They are ideal for remote areas because of the easy installation, small size and low weight¹³. The challenge with membranes in post combustion is the fact that the flue gas contains normally less than 15 % CO_2 which results in a low driving force for CO_2 permeation¹³.

1.2.1 Mixed Matrix Membranes

To enhance the properties of polymeric membranes, the concept of Mixed Matrix Membranes (MMM) is introduced. A MMM consists of an inorganic material incorporated into a polymer matrix in the form of micro- or nanoparticles¹³. Using different materials with different flux and selectivity allows the synergistic combination of polymers for easy processability and inorganic materials for superior gas separation performance. Targeted incorporation of a suitable inorganic material in a polymer matrix can enhance the physical, mechanical and thermal properties and stabilizes the membrane against changes in permeability with temperature¹¹. Some of the challenges that arise, include lower mechanical properties of the resulting MMM (brittle membranes), challenges in scaling-up the technology and higher cost compared to polymeric membranes^{11, 13}.

This project will focus on synthesizing a component to incorporate in a MMM. Graphene has been “dubbed” as a wonder material with a wide range of applications both scientifically and technological¹⁴. Graphene has shown great promise in several areas like energy production, catalysis, memory devices, 3D printing, drug delivery and gas separation and storage¹⁴⁻¹⁵. The following chapter will focus on how graphene can be used in membranes for carbon capture.

1.3 Graphene

Graphene was first isolated in 2004 and it is a carbon monolayer packed in a honeycomb lattice, as shown in Figure 1.3.1¹⁴⁻¹⁵. The sheet of sp^2 – carbons is 0.344 nm thin and is 200 times stronger than steel. Additionally, it exhibits flexibility and shows unique electronic and mechanical properties¹⁴⁻¹⁵.

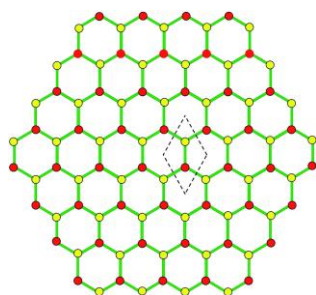


Figure 1.3.1: The structure of graphene. The dashed lines shows the unit cell of graphene¹⁴.

1.3.1 Graphene in CCS

Graphene has a high specific surface area and the planar geometry makes it amenable for functionalization or modification¹⁴. Because of the possibility of functionalization and its chemical, mechanical and thermal properties, graphene can overcome the shortcomings of already existing CO_2 adsorbents. Compared to other substances used as adsorbents in CO_2 capture, graphene is chemically inert and relatively stable. Especially in post combustion the stability of the adsorbent is important, as the flue gas contains large quantities of water and other contaminants like O_2 , SO_2 and NO_x ¹⁴. At the same time graphene is considered a “green material”, and has the potential to be easily accessible and scaled-up¹⁴.

In CCS-technology the graphene sheets can be used in the capturing process as a membrane by separating CO_2 from other substances. This can be done by functionalizing graphene with polymers that are CO_2 -philic and enhances the permeability of CO_2 , as shown in Figure 1.3.2¹⁶. By functionalizing graphene with CO_2 – philic groups the membrane will get a higher affinity to CO_2 than the other components (water, O_2 , SO_2 etc. in e.g. flue gas). The separation can then take place as a surface diffusion mechanism, as shown in Figure 1.2.2 ii¹³.

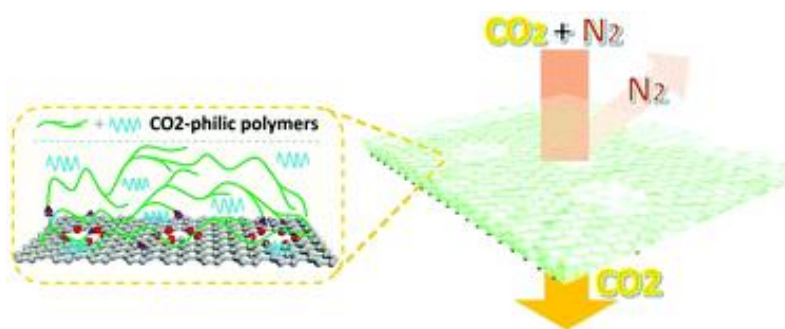


Figure 1.3.2: Functionalization of graphene sheet with polymers to make it more CO₂ – philic ¹⁶.

Functionalized graphene can be used as a membrane itself, but it can also be incorporated in a polymer matrix forming a MMM, as shown in Figure 1.3.3. The graphene sheets will act as additives in the membrane.

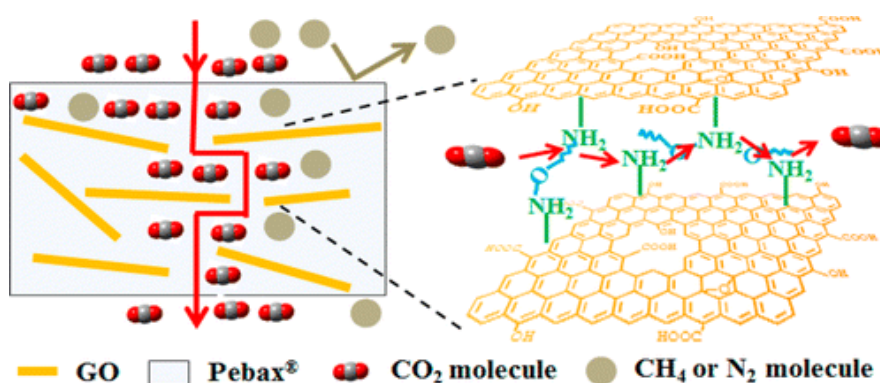


Figure 1.3.3: Graphene in a Mixed matrix membrane ¹⁷

1.3.2 Functionalization of graphene

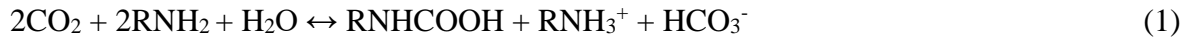
As mentioned in the previous section's graphene needs to be functionalized for numerous reasons. One reason to chemically modify graphene is to optimize the selectivity of the membrane through the attachment of appropriate chemical groups. This chapter will outline a strategy in identifying groups that can be suitable for enhancing the affinity of CO₂.

CO₂ is a polar and acidic gas and various groups have been identified as suitable candidates in promoting graphene's affinity to CO₂ once anchored ¹⁷. Ethylene oxide (EO) possess good affinity for polar gases and by functionalizing graphene with EO the solubility selectivity and the CO₂ selectivity can be increased ¹⁷. Solubility selectivity refers to one of the separation mechanisms mentioned in section 1.2. which is called solution diffusion and is shown in Figure 1.2.2i ¹⁸. This mechanism is based on differences in solubility of the gases that are separated.

Introduction

The gas targeted for separation solubilizes in the membrane while the other gases does not. This gas then diffuses across the membrane before it is desorbed under low pressure ¹¹.

Another method to increase the selectivity is to introduce basic groups, like amino groups in the membrane. In the presence of water the amino groups react with CO₂ as shown in equations 1, 2 and 3 ¹⁷.



Incorporating 2D materials in a MMM has shown great potential for enhanced CO₂ separation. Ismail *et al.* (2014) increased the diffusion selectivity by incorporation of layered silicate into the polymer matrix, ¹⁹ and Filiz *et al.*²⁰ increased the CO₂ solubility by incorporating PEG – functionalized polyoctahedral silsesquioxanes (POSS) into a poly-ether-*block*-amide (PEBAX) matrix. Wang *et al.* ²¹ incorporated polyaniline nanorods in the composite membrane and because of the reversible reaction with amino groups, CO₂ molecules could transfer quickly.

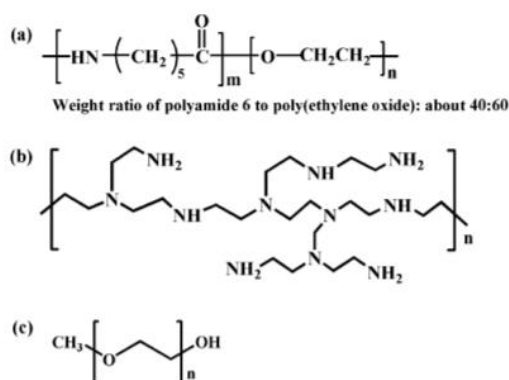
Overall this shows that in a polymer matrix amino groups can enhance the selectivity because of the reversible reaction with CO₂ and EO groups can enhance the solubility selectivity because of the excellent affinity for CO₂. In this master project graphene will be functionalized with EO groups before it is incorporated in an MMM to see if these groups are suitable for enhancing the CO₂ selectivity.

1.3.3 Graphene oxide and graphene in mixed matrix membranes

In the previous section some effects of incorporating 2D materials in MMMs were outlined. 2D materials like graphene and graphene oxide (GO) have also been studied for use in MMMs and in this section the results from some of these studies will be presented.

GO has been incorporated in MMMs for use in CO₂ capture several times. Dai *et al.* ²² incorporated imidazole functionalized graphene oxide into a PEBAX matrix and the selectivity for CO₂/N₂ was increased by 46 % compared to a pristine PEBAX membrane. Zahri *et al.* ²³ incorporated GO in a polysulfone polymer matrix and both the permeance of CO₂ and the CO₂/CH₄ separation was enhanced.

Li *et al.* ¹⁷ functionalized graphene oxide with both polyethylene imine (PEI) and polyethylene glycol (PEG) and incorporated in a Pebax matrix, all the structures are shown in Scheme 1.3.1.



Scheme 1.3.1: Structure of a) Pebax MH 1657, b) PEI, and c) PEG ¹⁷

This study showed that the separation of CO₂ was enhanced by incorporating graphene oxide functionalized with both PEG and PEI and in a Pebax matrix. The new multi-permselective membrane showed a longer, more tortuous path by incorporating GO nanosheets in the polymer matrix, the solubility selectivity was increased by incorporating PEG and the amino groups in PEI reacts reversibly with CO₂ and increases the CO₂ selectivity even more ¹⁷.

January 2020 Pazani *et al.* ²⁴ studied the influence of graphene based fillers in an PEBAX based MMM. This study compared the CO₂ permeability in neat PEBAX, PEBAX with graphene and PEBAX with graphene oxide (Fig 1.3.5). Incorporating 0.7 wt% graphene in the PEBAX matrix increased the CO₂ permeability by approximately 1.7 (from 26.51 to 44.78 Barrer) and by incorporating GO the CO₂ permeability increased by approximately 2.2 (from 26.51 to 58.96 Barrer). The results, as shown in the Robeson plot in Figure 1.3.4, showed that incorporation of both graphene and GO made the MMMs overcome the Robeson upper bound.

The Robeson plot shows that there is a trade-off between gas permeability and selectivity for gas separation in polymeric membranes. This was demonstrated by Robeson for the first time in 1991 and displayed in a upper bound curve ²⁵. In 2008 the upper bound was updated, ²⁶ and the research on membranes today aims to make membranes that reaches the targeted region, as shown in Figure 1.3.4.

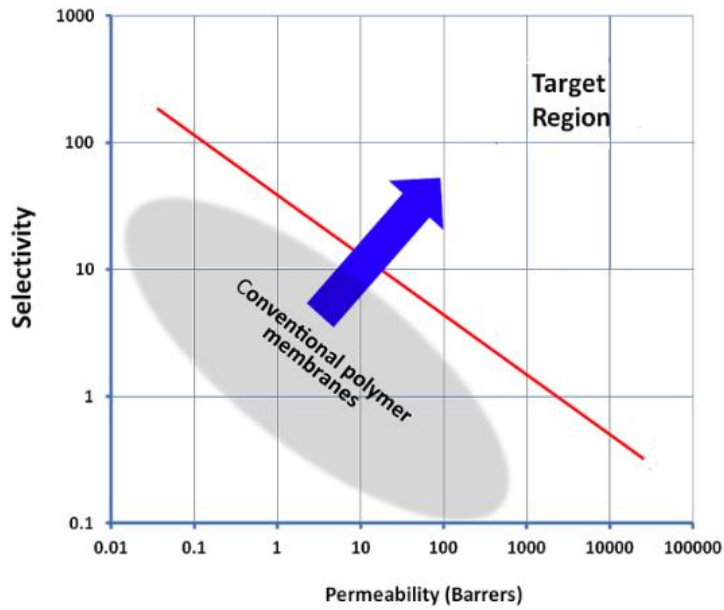


Figure 1.3.4: Robeson plot that shows the Robeson upper bound which new membranes tries to surpass ²⁷.

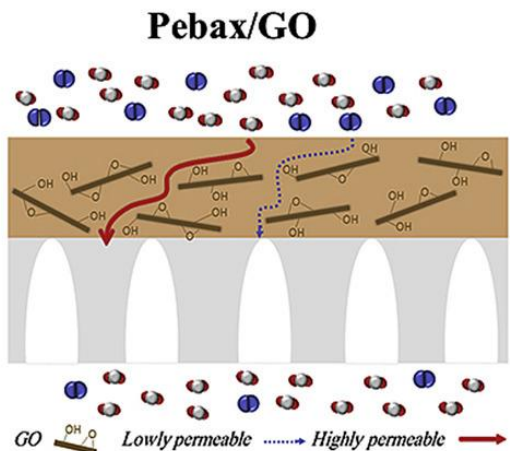
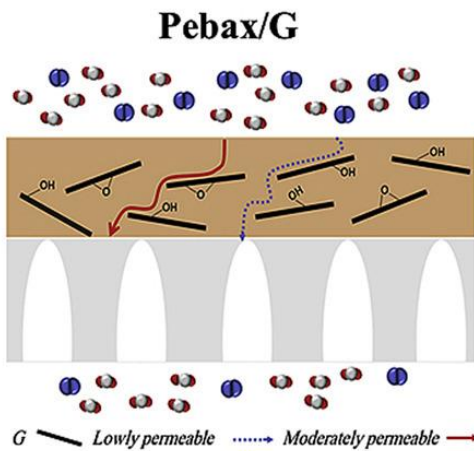
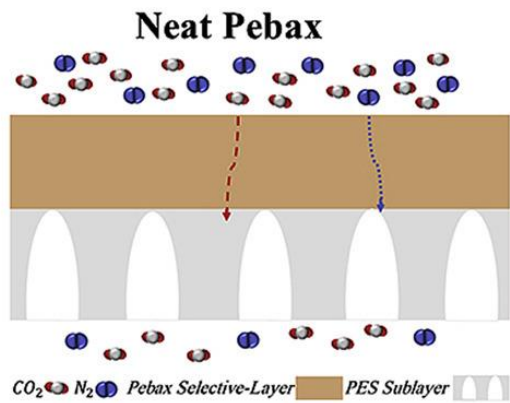
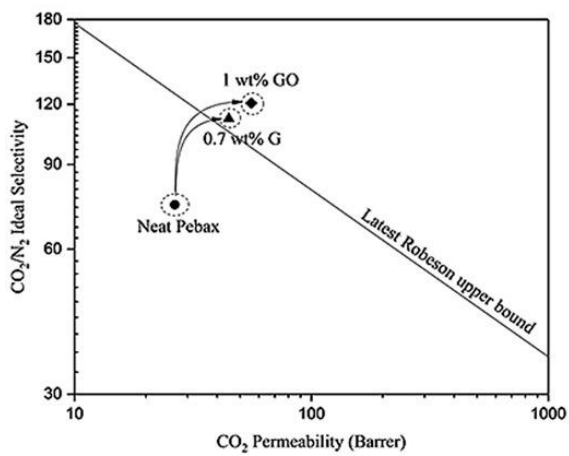


Figure 1.3.5: Schematic presentation of PEBAX, PEBAX with graphene and PEBAX with GO, and the Robeson plot of these ²⁴.

A lot of other studies on GO in MMMs for CO₂ capture have been performed, but this project will focus on the use of graphene and not GO in MMMs. Pristine graphene in MMMs are not studied as much as using GO. This is mostly due to the fact that GO has become the most abundant source of graphene-derivative in the material's ~15 years of spotlight since its isolation in 2004. Regardless, some studies on non-GO graphene have been published. Huang *et al.*²⁸ doped few-layer-graphene with nitrogen and incorporated the functionalized graphene in a PEBAX matrix. This showed an enhancement in the CO₂ permeability and the CO₂/N₂ selectivity. Pazani overcame the late Robeson upper bound incorporating graphene in a PEBAX matrix, as mentioned previously²⁴.

1.4 Organic chemistry and synthesis

At this stage, the role of graphene (and GO) is not completely elucidated in MMMs performance. Depending on the functionalization groups, graphene can play an active role on the selectivity. However, there is the possibility that the 2D material just assumes the role of a “nanofiller” in the polymer matrix and contributes to overall performance increase by simply increasing the permeability. Regardless of those two scenarios, in order for graphene to play an effective role the need for efficient dispersibility in the polymer matrix is evident. Graphene doesn't inherently possess any thermodynamic tendency to mix with the typical polymers comprising MMMs. As a result, if graphene is simply mixed with the polymer (either in solid state using e.g. an extruder or in a polymer solution prior to film casting) it will simply create large “graphite” aggregates, ultimately causing deterioration of mechanical properties. The most elegant way to overcome this and promote uniform distribution of graphene nanoparticles in a foreign medium i.e. polymer, is to chemically decorate graphene with groups that will have high affinity to that medium and/or prevent re-aggregation.

To enhance the permeability of the graphene sheets for carbon capture the sheets are to be functionalized with CO₂ – philic groups. There are several different methods for functionalization. It can be done by intercalation and both covalent and non-covalently, as shown in Figure 1.4.1¹³.

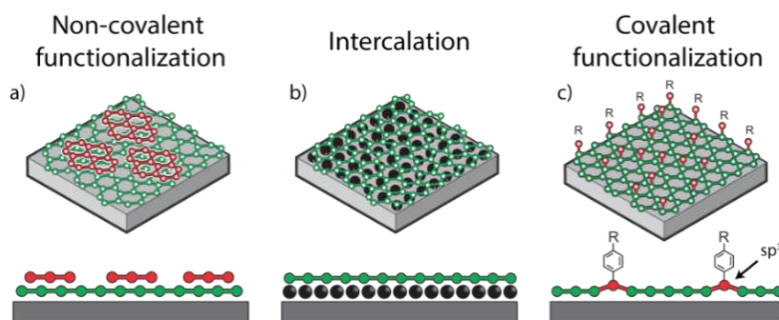


Figure 1.4.1: Non-covalent functionalization, intercalation and covalent functionalization of graphene

13

Since graphene has a conjugated π -system, π - π intercalation with other conjugated molecules is facilitated. When the modification of the graphene takes place non-covalently the sp^2 structure is retained. Covalent functionalization is, on the other hand, more stable and robust and allows for subsequent chemical processes²⁹. This project will focus solely on covalent functionalization of graphene.

1.4.1 Synthesis of graphene

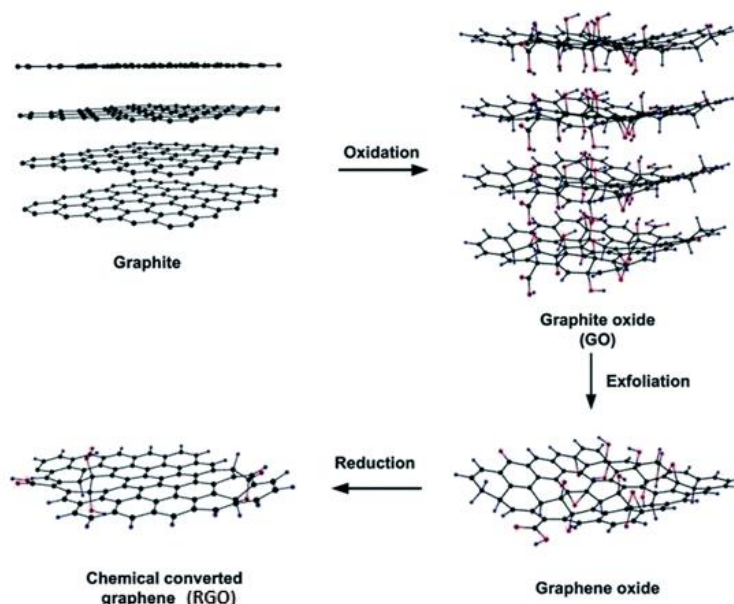
In general, there are two different routes for making graphene. It can either be done top-down or bottom up, where the top-down approach refers to breaking macroscopic structures into smaller ones, and bottom-up means building up graphene from carbon atoms³⁰. When graphene was first isolated in 2004 it was done by a so-called “micromechanical cleavage”, a top-down approach where scotch tape was used to exfoliate graphite³¹. Using this method pristine graphene can be obtained, but the yield is an extremely small amount and cannot be used for anything but fundamental research³².

A common and environmental-friendly top-down approach is to exfoliate graphene from graphite. This can be done by, for example, sonication of graphite in suitable organic media³³. Tour *et al.*³⁴ isolated graphene monolayers with graphite dispersed in *o*-DCB and Bourlinos *et al.*³⁵ dispersed graphite in several different organic solvents, including Perfluorinated aromatic molecules, pyridine and chloroacetate, by using extended bath sonication and subsequent centrifugation. Coleman *et al.*³³ describes a method where graphene is exfoliated by sonication of graphite flakes in *N*-methyl-2-pyrrolidone (NMP) for 30 min before centrifugation and collection of the supernatant.

Using a top-down approach it is challenging to produce large and defect free pieces of graphene mainly due to the inherent statistical nature of the production method, yielding inconsistent products. For some applications, like electronic devices, large pieces of graphene are required. For such applications bottom-up techniques have been deemed more suitable. The bottom-up

approaches consists mainly of epitaxial growth of graphene on a substrate by chemical vapor deposition (CVD), plasma enhanced CVD (PECVD), solvothermal synthesis, pyrolysis, and thermal decomposition of silicon carbide (SiC) wafer under ultrahigh vacuum conditions ³⁰.

The most popular top-down approach to produce graphene is *via* oxidation of graphite. First graphite is oxidized to graphite oxide, which readily exfoliates to GO and then GO is reduced to graphene or the more accurately termed, reduced graphene oxide (RGO) (Scheme 1.4.1). Common oxidation methods are the Brodie method, the Staudenmaier method and the Hummers method³⁶, and reduction is done with strong reducing agents like hydrazine, dimethylhydrazine, NaBH₄, and hydroquinone. The disadvantage of using this method is that the graphene produced after reduction still contains many defects therefore needing the distinction of RGO rather than graphene ³².



Scheme 1.4.1: Production of graphene through oxidation of graphite, exfoliation of graphite oxide and reduction of graphene oxide ³⁷.

CVD has been the most prominent bottom-up production method of graphene. Using CVD it has been possible to produce graphene with a small number of defects over a large area ³³. The problem with this method is that it is challenging to scale up for bulk production of graphene. By contrast wet chemical methods, outlined in Figure 1.4.2. have shown to be scalable for producing graphene suitable for chemical functionalization ³².

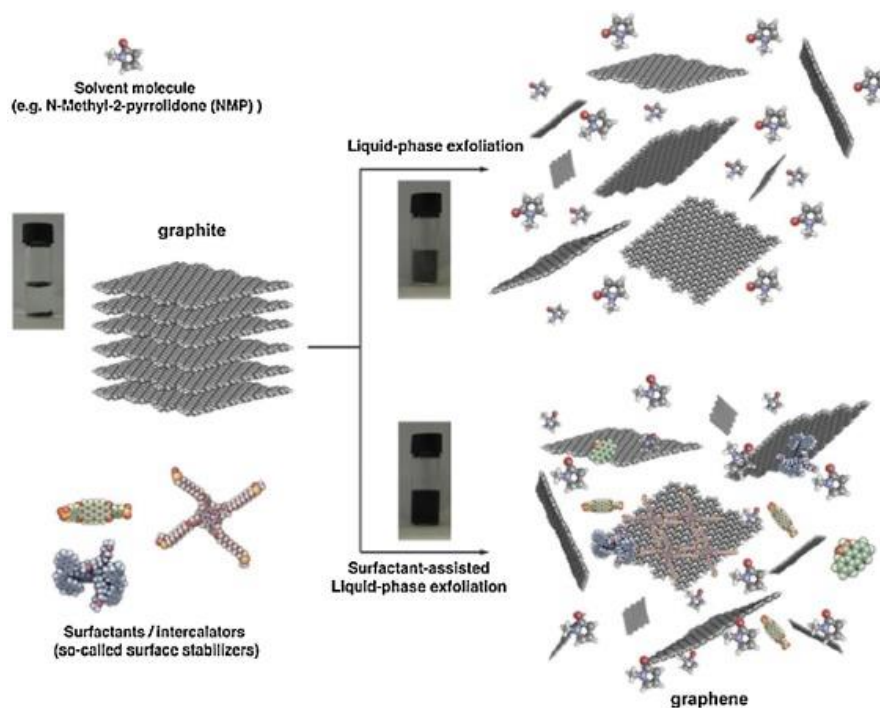


Figure 1.4.2: Schematic representation of liquid phase exfoliation (LPE) with the presence of surfactant molecules (bottom right) and in absence of surfactant molecule (top-right) ³².

In liquid phase exfoliation (LPE), graphite is dissolved in a suitable medium and an exfoliation process mediates to separate the individual graphene layers. To exfoliate graphene, the Van der Waals interaction between the sheets needs to be overcome. The estimated surface energy of graphene is 46.7 mN/m, ³⁸ and by using exfoliation agents with a surface energy around 40 mN/m the interfacial tension between the solvent and the graphene layer is minimized. Some solvents that can be suitable is N-methylpyrrolidone (NMP, 40 mN/m), N,N'-dimethylformamide (DMF, 37.1 mN/m), γ -butyrolactone (GBL, 35.4 mN/m), and ortho-dichlorobenzene (*o*-DCB, 37 mN/m) ³². Graphite was exfoliated using LPE for the first time in NMP ³³. The graphene that was produced was considered to be pristine graphene, but the yield was only 1 wt % and the concentration of the produced suspension only 0.01 mg/mL. Early attempts at LPE using *o*-DCB, produced dispersions with 0.03 mg/mL, ³⁴ pentafluorobenzonitrile produced 0.1 mg/mL, ³⁵ and benzylamine produced 0.5 mg/mL ³⁹. Surfactants have also been successful in assisting the LPE. Addition of melissic acid in NMP increased the exfoliation yield by 200 % and produced nearly 50 % monolayer graphene ³². The problems by using a surfactant molecule is that there can be residual molecules between the graphene sheets that will affect the properties of the produced carbon nanomaterial ⁴⁰. Some *et al.* ⁴¹ introduced binol salt as a stabilizing surfactant during reduction of GO. The binol salt was completely removable and the properties of graphene were not affected.

Introduction

There have been several attempts to promote the LPE process, but the challenge remains the poor quality and the statistical nature of the produced graphene, compared to bottom up methods. However, it is the second most scalable technique behind GO (and reduced GO) and offers higher quality graphene using easily accessible equipment ³².

Electrochemical exfoliation of graphene and supercritical fluid exfoliation are two alternative routes for wet chemistry production of graphene. As summarized in Table I, the first one gives high yields, has low production time, is cost effective, has high processability, is environmentally benign, scalable and gives yield graphene with adequate electronic properties. The disadvantages include mild oxidation and inhomogeneous thickness of the graphene flakes. The supercritical fluid exfoliation is a potentially fast method and is easy to process, but it gives a low yield of single graphene layers and the electronic properties are affected ³².

Table I: Summary of advantages and disadvantages associated with graphene production by wet chemical routes ³².

Graphene exfoliation methods	Advantages	Disadvantages
Liquid-phase exfoliation	High-quality Simple preparation method Potentially scalable Non-oxidative route	Low yield of thin graphene layers Small flake size (<5 μm) Limited dispersability Limited processability
Graphene from graphite oxide	High yield High dispersability High processability Scalable method	Poor quality and/or defective structures Potentially explosive process Time consuming Use of toxic chemicals Poor electronic properties
Electrochemical exfoliation	High yield Fast production Cost effectiveness High processability Environmentally benign Scalable Good electronic properties	Slight oxidation Inhomogeneous flake thickness
Supercritical fluid exfoliation	Potentially fast method Ease of processing	Low yield of thin graphene layers Electronic properties are affected

To summarize, the several different wet chemical routes to produce graphene possess both advantages and disadvantages. In this project liquid-phase exfoliation will be used because the method is facile and produces adequate quality and sufficient quantities of graphene to be used for chemical functionalization

1.4.2 Chemistry on graphene

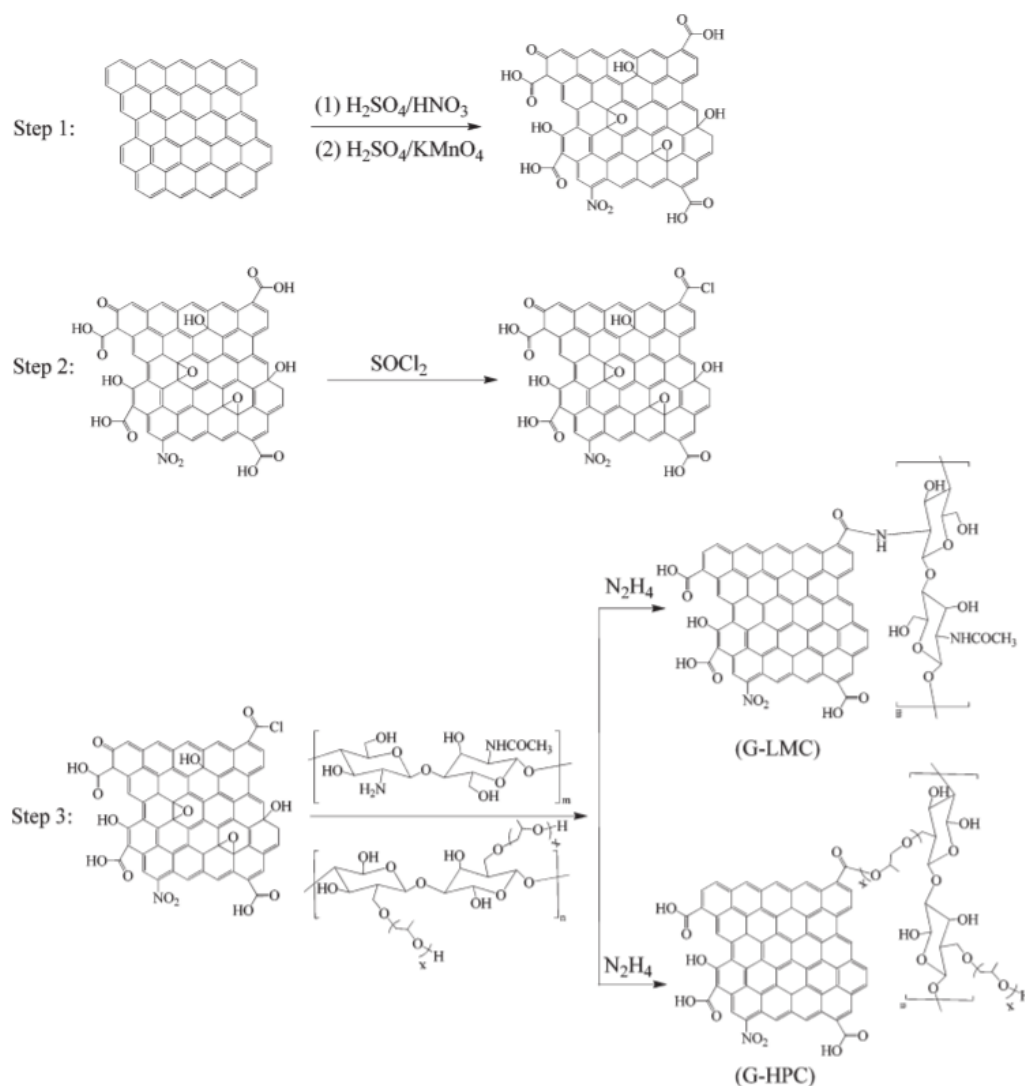
In the following section different ways to functionalize graphene will be presented. Some of the routes will only be briefly mentioned, while some will be presented more detailed. In the end of the section the process that will be used in this project will be presented.

Introduction

As explained, the efficient incorporation of graphene in the growing polymer-based gas separation industrial processes⁴² requires chemical functionalization. This can be done in several ways. Three general routes for covalent functionalization exist. One involves the formation of covalent bonds between free radicals or dienophiles and C=C bonds of pristine graphene and the second one involves typical classic acid-base chemistry between organic functional groups and the carboxylic groups of graphene oxide⁴³. The third route involves doping of the graphitic lattice with inorganic elements, which have shown to have a strong impact on the physical and chemical properties of graphene⁴⁴. Such processes include hydrogenation,⁴⁵⁻⁴⁶ nitrogenation,⁴⁷ oxygenation,⁴⁸ and halogenation⁴⁹.

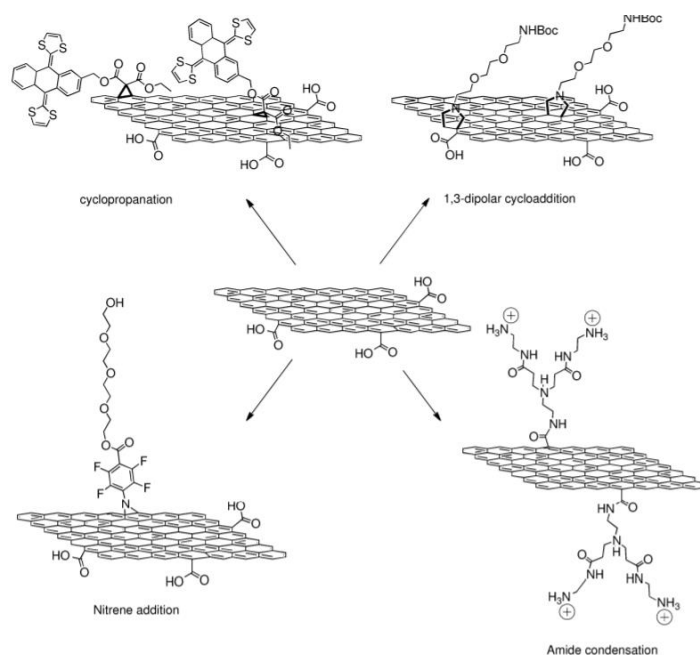
Classic organic reactions can also be used in the functionalization of graphene. Yao *et al.*⁵⁰ functionalized graphene with polythiophene through a classic Suzuki coupling reaction. Yang *et al.*³⁶ covalently functionalized graphene oxide with polysaccharides through an esterification reaction. GO was reacted with SOCl₂ at 80 °C for three days to convert the carboxyl-group to acyl-chloride and GO-COCl was obtained. GO-COCl was then dispersed in DMF containing hydroxypropyl cellulose (HPC) and was left at 120 °C for two days before it was washed and dried and GO-HPC was obtained. Finally, the GO-HPC was reduced with hydrazine for three days. The procedure is shown in Scheme 1.4.2.

Introduction



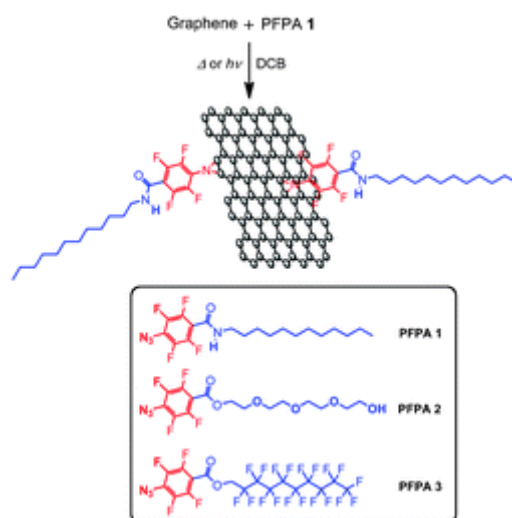
Scheme 1.4.2: Preparation of graphene functionalized with polysaccharides ³⁶.

In 2010 Prato *et al.* ⁵¹ functionalized graphene by a 1,3-dipolar cycloaddition reaction of in-situ generated azomethine ylides. This reaction, shown in Scheme 1.4.3, has proceeded successfully with both NMP and DMF as the exfoliating agent ⁵¹. Zhang *et al.* ⁵² functionalized graphene with porphyrin through a cycloaddition reaction. In Scheme 1.4.3 other functionalization routes like cyclopropanation, nitrene addition, and amide condensation are also presented ⁵³.



Scheme 1.4.3: Different ways to functionalize graphene ⁵³.

Azide chemistry has also been used functionalizing graphene ⁵⁴. Liu and Yan attached perfluorophenylazides covalently onto graphene using *o*-DCB as the exfoliating agent and the reaction was carried out at 90 °C for 72 hours (Scheme 1.4.4).



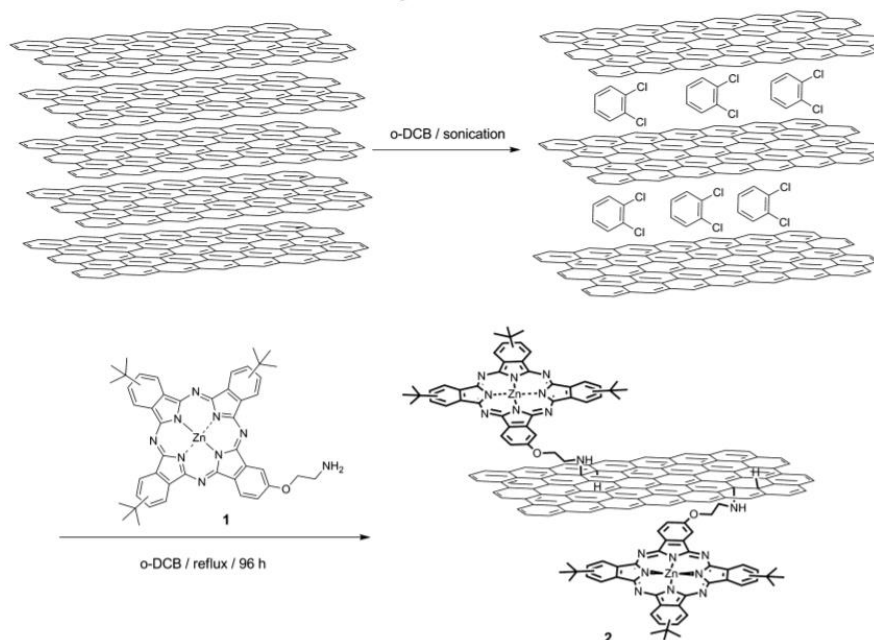
Scheme 1.4.4: Functionalization of pristine graphene with perfluorophenylazides ⁵⁴.

Small acetylene groups can be anchored on to the graphene, *via* azide chemistry and can act as anchoring sites for conjugated polymers. Castelaín *et al.* ⁵⁵ used this method to anchor polyfluorene onto graphene.

Karousis *et al.* ⁵⁶ covalently functionalized primary amines on to carbon nanomaterials by a direct nucleophilic addition. The graphene was prepared by sonication in *o*-DCB using a tip sonicator for $t = 15$ min, followed by ultrasonic bath treatment for another $t = 2.5$ h. the

Introduction

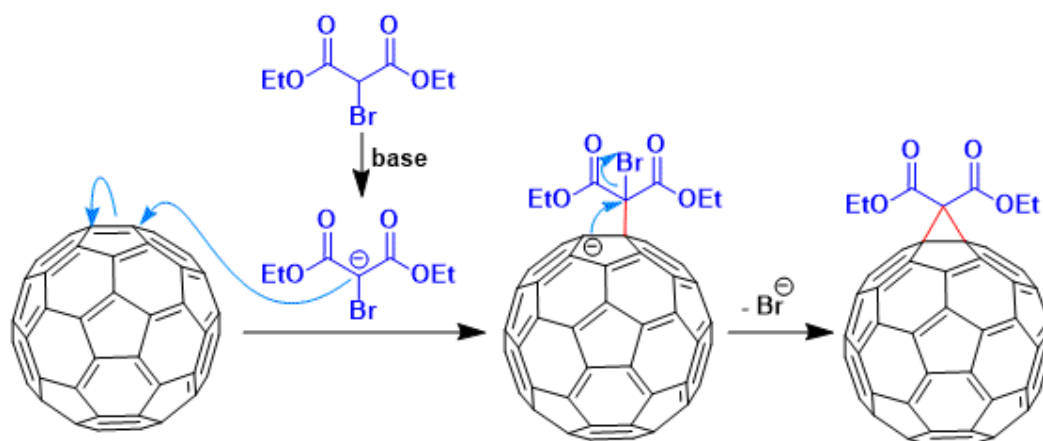
functionalization was done by treating the exfoliated graphene dispersed in *o*-DCB with ZnPc at 120 °C for 96 hours (Scheme 1.4.5) before it was filtered and washed with *o*-DCB, methanol and DCM.



Scheme 1.4.5: Covalent functionalization of graphene with ZnPc in *o*-DCB ⁵⁶.

Another way to functionalize graphene that has proven to be efficient, is the use of aryl diazonium salt reaction ⁵⁷. This can prevent reaggregation because of steric repulsion between the graphene layers when bulky aryl moieties is incorporated on the graphene sheets ⁵⁸ and shows potential as an intermediate step for further functionalization which can lead to further enrichment of functional groups decorating the carbon nanomaterial ⁵⁹.

The Bingel reaction was first discovered by Carsten Bingel in 1993 as a fullerene cyclopropanation reaction. Methanofullerene is cyclopropanated with a bromo derivative of diethyl malonate in the presence of a base, as shown in Scheme 1.4.6 ⁶⁰.



Scheme 1.4.6: Bingel reaction mechanism. Cyclopropanation of methanofullerene with a bromo derivative of diethyl malonate in the presence of a DBU ⁶⁰.

In carbon nanohorns (CNHs) the malonyl moieties have been incorporated using Bingel reaction conditions, and microwave – assisted organic chemistry have been successfully used to covalently attach various organic groups ⁶¹. The use of microwave-assisted synthesis in functionalization of CNHs has shown great potential, by being a simple and reliable procedure that is time efficient in comparison to the conventional method. If this method can be combined with solvent-free procedures reducing environmental footprint and applying green chemistry conditions ⁶¹. Imahori *et al.* ⁶² combined these methods and efficiently functionalized the side walls of SWNTs.

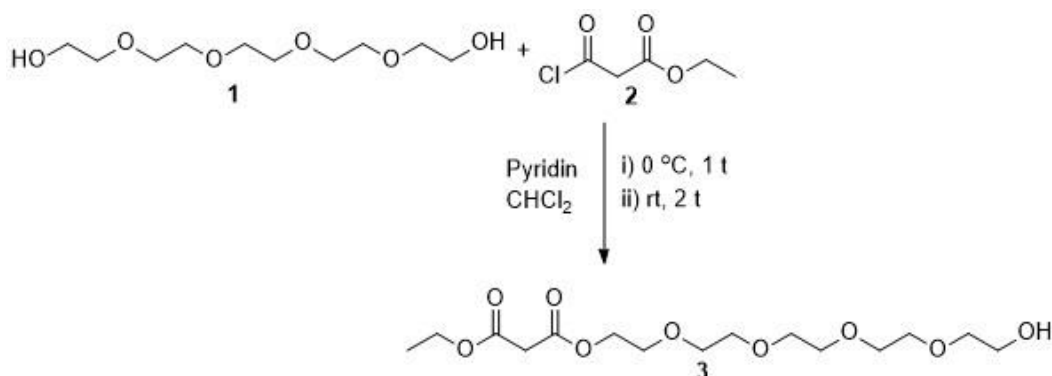
For this project this microwave-assisted Bingel reaction is used to functionalize graphene with 2-(2-(2-ethoxyethoxy)ethoxy)ethylethylmalonate. The reasoning is the scalable production of the malonate starting material and the shortened reaction times afforded by the microwave irradiation.

1.4.3 Synthesis of malonate

One of our novel graphene hybrids with ethyleneoxide addends, was recently synthesized in our group, ⁶³ and was particularly promising as a material that would disperse well in a PVA matrix. The process to design and synthesize the graphene hybrid, consists of the appropriate modification of a triethyleneglycol analogue (containing the desired ethylene oxide group) to yield a molecule suitable for covalent attachment onto the graphitic backbone. In order to attach the triethyleneglycol functional unit to graphene, the Bingel-Hirsch cyclopropanation reaction was chosen ⁶⁰. This process requires the presence of a malonate unit which will act as the anchoring molecule to the carbon nanomaterial. There are several examples of the synthesis of malonate analogues in the literature.

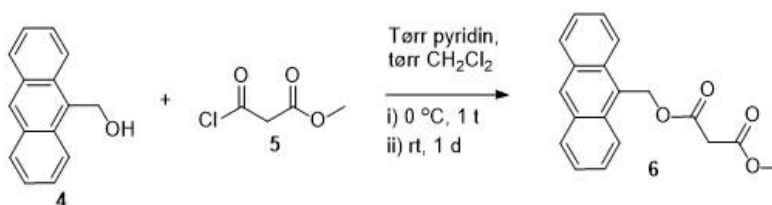
Introduction

Ethyl-(14-hydroxy-3,6,9,12-tetraoxatetradecyl)malonate (**3**) was synthesized by Trinh *et al.*⁶⁴ in 65 % yield through a mono-esterification of pentaerythritol (**1**) with ethylmalonylchloride (**2**) in the presence of pyridine, as shown in Scheme 1.4.7.



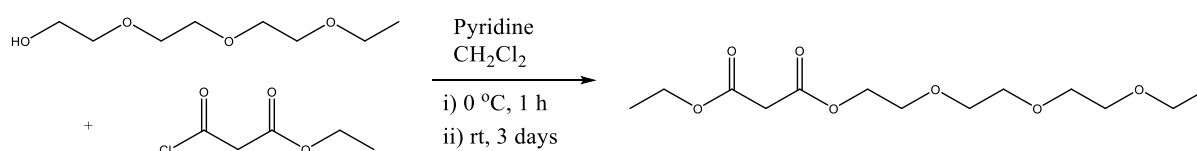
Scheme 1.4.7: Synthesis of ethyl-(14-hydroxy-3,6,9,12-tetraoxatetradecyl)malonate (**3**) through an monoesterification of pentaerythritol (**1**) with ethylmalonylchloride (**2**).⁶⁴

Antracen-9-ylmethylmethoxymalonate (**6**) was synthesized by Economopoulos *et al.*⁶¹ by esterification through a nucleophilic acyl-substitution of antracen-9-ylmethanol (**4**) with methyl-3-chloro-3-oxopropanoate (**5**) in the presence of dry pyridine, as shown in Scheme 1.4.8.



Scheme 1.4.8: Synthesis of Antracen-9-ylmethylmethoxymalonate through an esterification of antracen-9-ylmethanol med ethylmalonylchloride (**2**).⁶¹

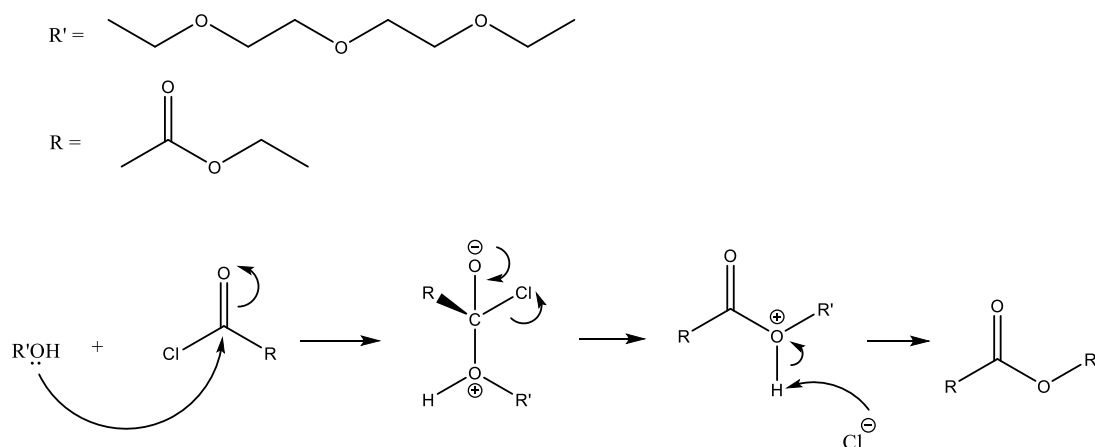
In this thesis 2-(2-(2-ethoxyethoxy)ethoxy)ethylethylmalonate will be synthesized from 2-(2-(2-ethoxyethoxy)ethoxy)ethane-1-ol and ethyl-3-chloro-3-oxopropanoate, as shown in Scheme 1.4.9⁶³.



Scheme 1.4.9: Synthesis of 2-(2-(2-ethoxyethoxy)ethoxy)ethylethylmalonate from 2-(2-(2-ethoxyethoxy)ethoxy)ethane-1-ol and ethyl-3-chloro-3-oxopropanoate.

Introduction

The reaction type is an esterification going through a nucleophilic acyl substitution where the nucleophile, glycol 1, replaces the leaving group, the chloride, on malonylchloride 2, as shown in Scheme 1.4.10.



Scheme 1.4.10: Mechanism for synthesis of 2-(2-(2-ethoxyethoxy)ethoxy)ethylethylmalonate by an esterification of 2-(2-(2-ethoxyethoxy)ethoxy)ethane-1-ol and ethyl 3-chloro-3-oxopropanoate through a nucleophilic acyl substitution.

1.4.4 Microwave-assisted chemistry

Microwave-assisted chemistry has shown to have a lot of advantages since it was first applied in 1986. Compared to traditional heating methods microwave reactors provide shorter reaction time, better reproducibility, reduced side reactions and they are easy to use⁶⁵. Microwaves generate energy as the wave moves and this energy can interact with for example a solvent and release energy. There are both monomode reactors and multimode reactors where in the monomode reactor the microwave energy produced is at a single wavelength and in the multimode there are several microwavelengths generated. In the monomode the heat distribution is homogenous, but in the multimode “hot” and “cold” areas are created and stirring of the reaction mixture is essential.

Microwaves only penetrate a small depth into the sample, so continuous-flow processing needs to be used in order to expose the whole sample for the microwaves. Choosing solvents for use in microwave chemistry is of great importance. Generally polar solvents interact well with microwaves, and non-polar solvents do not. In polar solvents the molecular rotation is increased, and heat is released when it is exposed to microwaves.

Aim of the thesis

This master project is part of a larger international ACT-ERANET project on CCS. The Norwegian side of the project is tasked with synthesizing functionalized graphene derivatives in order to be tested on MMM. This thesis focuses on the synthesis of novel graphene derivatives in suitable quantities in order to be sent to our collaborators at NETL (USA) for incorporation in a polyvinylamine (PVA) matrix and tested for overall performance (selectivity/permeability). The functional group of triethylglycol was identified as a potential group offering graphene dispersibility in the same solvents as PVA and good dispersibility in the polymer matrix. The initial quantities required to conduct testing is ~50mg of functionalized product. A typical cyclopropanation reaction using malonates yields approx. 1-2 mg of functionalized product. The thesis was, initially, focused on identifying different functionalization techniques to ascertain which one is better for the production of the required quantity. However due to the COVID 19 outbreak and the time constraints, the focus of the thesis shifted on the use of the tried and tested cyclopropanation reaction due to two reasons. The reaction takes place under microwave irradiation significantly reducing time and the synthesis of the required malonate was streamlined (different reaction conditions would require the synthesis of different anchoring groups on the triethylene glycol). During the numerous reactions required to achieve the desired quantity of functionalized product, attempts were made to identify optimum reaction conditions.

2. Results and discussion

Initially the task at hand was to synthesize the malonate derivative in order to be attached onto graphene. 2-(2-(2-Ethoxyethoxy)ethoxy)ethylmalonate was synthesized as a yellow/orange oil five times. In all the batches synthesized, yields of ~80% or above, were observed. Individual yields can be seen in the Experimental section 5.1. NMR (Fig 8.1.1 – Fig 8.1.9) showed that the products was clean. Complete peak assignment is listed in Table II. The MS showed Na as a trace element (Appendix 8.2). The product was washed with brine, and it seems like the Na⁺ ion was not completely washed away. The malonate was presumed to be pure enough to be used in the functionalization of graphene.

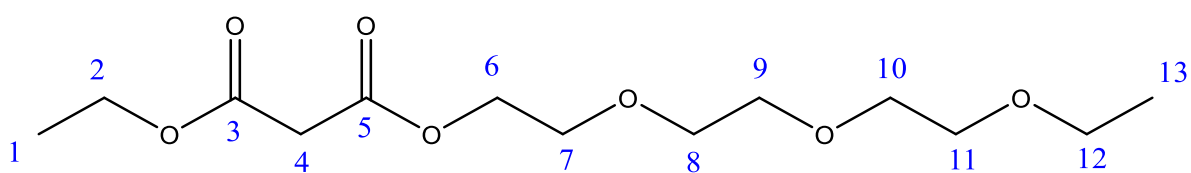


Figure 2.1: 2-(2-(2-Ethoxyethoxy)ethoxy)ethylmalonate (KE-ME1-5) with all the positions numbered. The chemical shift along with coupling constants, integrals, and multiplicity is shown in Table 2.1.

Table II: Chemical shifts along with coupling constants, integrals, and multiplicity for KE-ME1-5 assigned to the positions shown in Fig. 1.2

Position in Fig. 2.1	δ_{H} [ppm]	Multiplicity	Integral [#H]	J [Hz]	δ_{C} [ppm]
1	1.23-1.19	t	3	6.96	14.06
2	4.23-4.18	q	2	7.02	61.55
3	-	-	-	-	166.65/166.46
4	3.41	s	2	-	41.49
5	-	-	-	-	166.65/166.46
6	4.32-4.29	t	2	4.84	66.64
7	3.73-3.58	m	2	-	68.87
8	3.73-3.58	m	2	-	69.82/70.60
9	3.73-3.58	m	2	-	70.63/70.74
10	3.73-3.58	m	2	-	70.63/70.74
11	3.73-3.58	m	2	-	69.82/70.60
12	3.55-3.50	q	2	6.94	64.58
13	1.30-1.27	t	3	7.17	15.16

To be able to functionalize graphene, graphene of high quality must be obtained. In this project several different exfoliation routes have been tested. All of them have been done using a tip-sonicator. Literature (Coleman *et al.*³³) predicts that sonication in NMP is the most efficient and it has been used in our lab with successful and repeatable results. According to the same studies

the sonication output power is crucial to the production of high yield graphene dispersion. In this project the sonication will be done in NMP.

After sonication, the exfoliated graphene creates stable dispersions for several months. The non-exfoliated graphene of large graphitic nanoparticles (comprised of >15 graphene layers) can be easily separated *via* centrifugation (4000 rpm, 5mins). Filtration, through a 0.45 μ m PTFE filter removes the solvent and affords the produced exfoliated graphene. NMP exfoliates graphene through a “wedge-like” approach as the planar pyrrolidone ring is inserted between the graphene layers of graphite. NMP is stabilized onto the nanocarbon through non-covalent interactions preventing re-aggregation and “causing” the long-term stability of the produced dispersion. Since visual confirmation of stable dispersions is an important aspect of reaction success in graphene chemistry (equivalent to TLC in classic organic synthesis) there is a need to certify that the observed dispersions we obtain come indeed from the induced solubility enhancement of the organic addend decoration and not from other factors such as residual exfoliating agent still attached non-covalently to exfoliated graphene. To this end, a series of “blank” experiments were performed were after exfoliation, centrifugation and filtration, the obtained graphene was redispersed in NMP, *o*-DCB and DCM and bath-sonicated for $t = 30$ sec. In Figure 2.2 these results are shown.

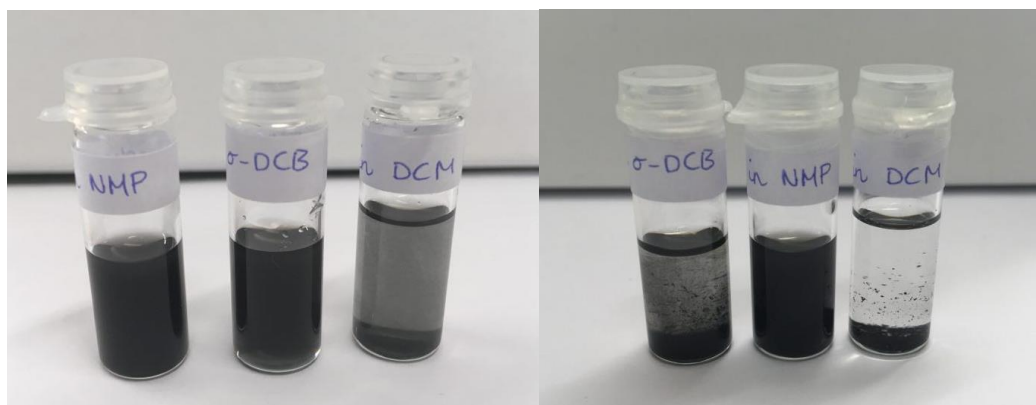


Figure 2.2: Graphene dissolved in NMP, *o*-DCB and DCM, immediately after sonication (left) and after after 48 hours (*o*-DCB) and 24 hours (NMP and DCM) (right).

Graphene is poorly dissolved in DCM and well dissolved in NMP and *o*-DCB. A close look can reveal that NMP is slightly darker than *o*-DCB. After 24 hours the graphene is almost completely precipitated in DCM and there has also been some precipitation in *o*-DCB after 48 hours. The graphene dissolved in NMP remains unaffected. Since the functionalization reaction

Results and discussion

usually takes place immediately after producing exfoliated graphene, both NMP and *o*-DCB seem to be suitable solvents of graphene functionalization.

The samples of graphene shown in Figure 2.2 have been prepared using the Bandelin SONOPULS HD2070 70W with the flat head probe (VS 70T) at 90 % (63 W), in icebath for $t=30$ min. Comparing sonication at 63 W and at 28 W was done, and the resulting dispersion after centrifugation, are shown in Figure 2.3. Using 63 W gives a darker color than 28 W. This indicates that more graphene has been exfoliated at 63 W, than at 28 W. To this end, the higher intensity setting on the tip sonicator will be used for the supply of our graphene starting material.



Figure 2.3: Graphene prepared in a tip sonicator in icebath for 30 min at respectively 28 Watt (40 %) and 63 Watt (90 %).

As mentioned above, visual confirmation is an important aspect providing quick feedback on graphene and carbon nanotube reaction. To see if any functionalization has taken place it can be useful to look at the color of the solution. As shown Figure 2.2 exfoliated graphene is not stable in DCM.

Functionalization of graphene involves the addition of reagents in a hermetically sealed vial and exposing them to microwave irradiation. The vial is sealed with a cap bearing a septum which allows for accurate pressure measurement through a sensor. As microwaves affect dipoles, some solvents e.g. H_2O react harshly under microwave irradiation and can cause vial explosions if pressure is not monitored constantly. A typical functionalization reaction consists of the following basic steps. The reaction mixture is subjected to microwave irradiation (or

conventional heating in an oil bath) for the specified amount of time. Then the mixture is allowed to reach RT and then filtered through a 0.45 μ m PTFE membrane filter. Reacted and unreacted graphene will remain on the filter. Careful washing of the solid product using DMF, MeOH and finally DCM is performed to remove any remaining reagents until the filtrate is clear-colored. The final solvent is preferentially DCM due to the solvent's low boiling point. The solid material in the filter is then redispersed in the solvent of choice (in this case DCM) and subjected to low-power bath sonication for $t = 30$ sec. Finally the mixture is centrifuged at 4000 rpm for $t = 5$ mins and the supernatant is collected as the unfunctionalized or partly functionalized graphene is discarded in the precipitate. Centrifugation can also “control” the quality and quantity of the afforded material as lower or higher rpm or shorter/longer times can afford higher quantity/lower quality or lower quantity/higher quality product respectively.

When graphene is functionalized it is stable in common organic solvents such as DCM. Figure 2.4 shows sample KE-GM1 three months after functionalization. KE-GM1 is obtained using a the microwave-assisted Bingel reaction. The different parameters in the reaction are listed in Table IX in the appendix. The color of the solution has not changed which means that the graphene is stabilized due to robust covalent bonds formed .



Figure 2.4: Sample KE-GM1 three months after functionalization.

Spectroscopic evidence of covalent functionalization comes from microRAMAN spectroscopy. A short summary describing the technique and its value in carbon nanomaterials' characterization, can be found in the experimental section. A solution containing KE-GM10, 11 and 12 in DCM was analyzed by Raman spectroscopy. The Raman spectra (Fig 2.5) shows successful functionalization of graphene with the malonate. The so-called I_D/I_G ratio for the exfoliated starting material is ~ 0.25 indicating a number of sp^3 “defects” in the graphitic

backbone as a result of tip sonication. The small shoulder at $\sim 1630\text{ cm}^{-1}$ is also associated with the presence of defects. Once the reaction has taken place in the microwave, the I_D/I_G ratio is now $\sim 0,63$ indicating that the defect sites (sp^3 -hybridized carbons) are considerably more, verifying spectroscopically that a chemical reaction has taken place on the graphitic backbone. As the produced exfoliated graphene will be used for MMM experiments, several reactions were “mixed” to produce the characterization sample in order to determine more accurately the material’s “bulk properties”.

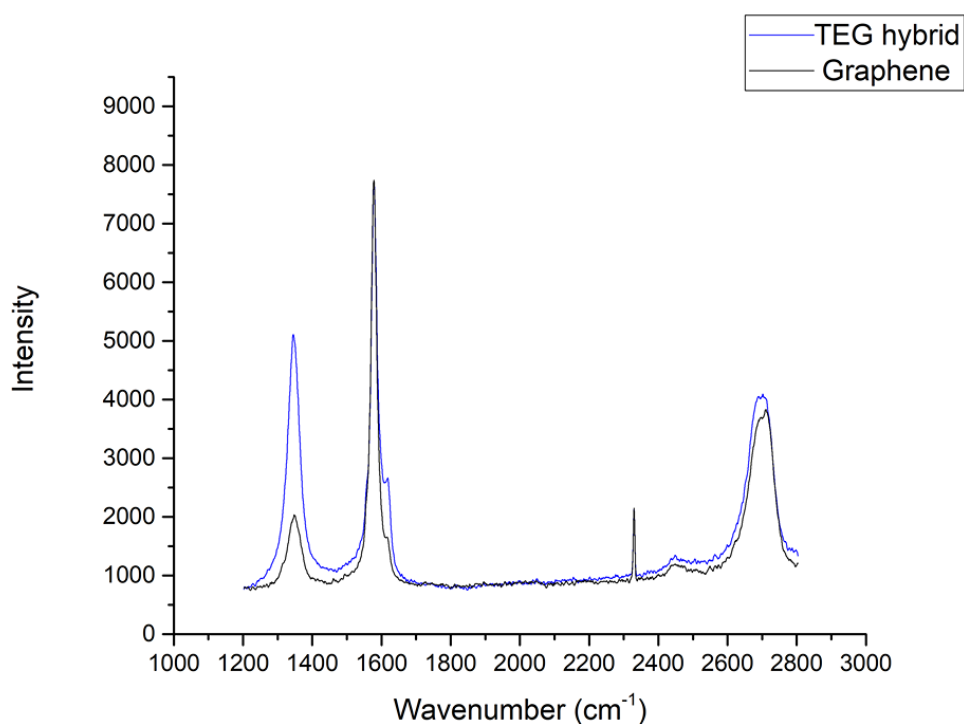


Figure 2.5: Raman – spectra of exfoliated graphene (black line) and graphene functionalized with 2-(2-(2-ethoxyethoxy)ethoxy)ethylethylmalonate (blue line). The sample of TEG hybrid measured, is a mixture of several experiments.

Another indication that the functionalization has been successful can be seen by comparing the IR-spectra of the malonate with the IR-spectra of functionalized graphene. Comparing IR-spectra of the malonate (Fig 2.6) and of KE-GM18 (Fig 2.7) they both have a significant peak at around 1700 cm^{-1} which indicates a C=O stretch, and some peaks in the region $2800\text{-}2900\text{ cm}^{-1}$ which indicates aliphatic C-H stretch. If functionalization did not take place the sample KE-GM18 would not have had these peaks.

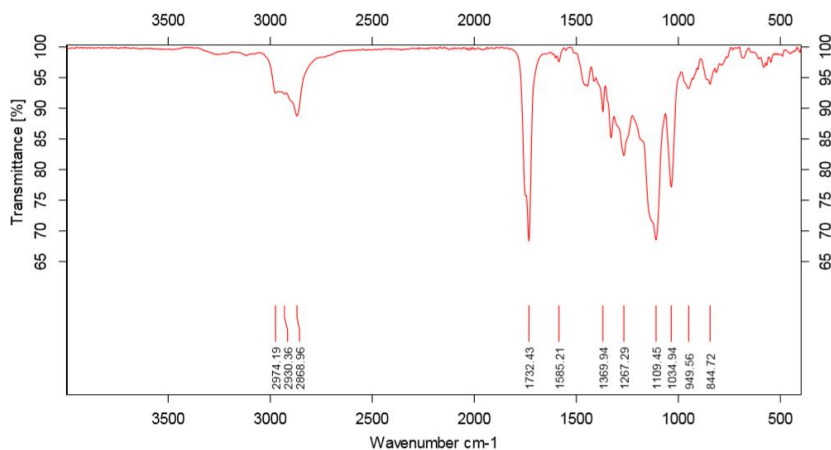


Figure 2.6: IR-spectra of 2-(2-(2-ethoxyethoxy)ethoxy)ethylethylmalonate.

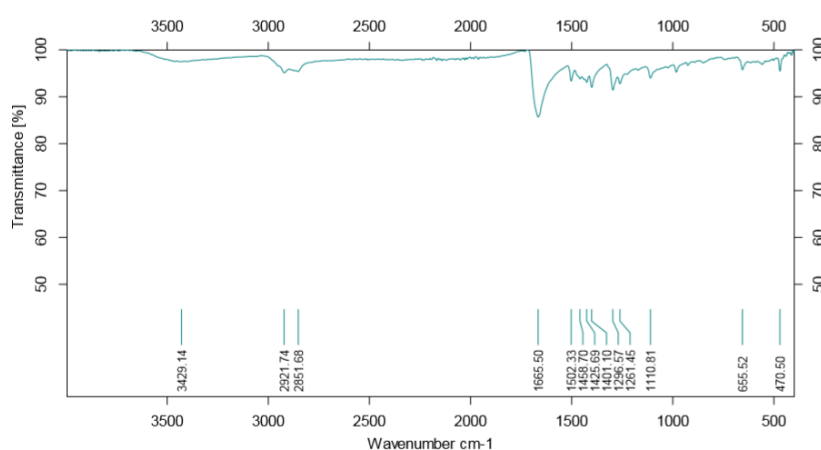


Figure 2.7: IR-spectra of graphene functionalized with the malonate. Sample KE-GM18


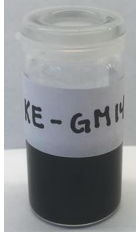




In order to produce the required amount for the project, several reactions need to be performed. Literature has shown that the reaction cannot scale properly³⁹. In addition, lab-scale microwave reactors offer limited possibilities for reaction volumes. As a result, multiple reactions need to be performed to obtain the required ~50 mg. Each reaction is assumed to produce ~1-2 mg of functionalized material. This can be, roughly, calculated by drying and weighing on a thermogravimetric analysis instrument scale (accuracy 0.001 mg) of a certain volume of dispersion and then extrapolate the results for other dispersion volumes. Other measuring techniques include UV-Vis spectroscopy through the use of a calibration curve for graphene. For our use, visual confirmation of the dispersion is sufficient.

For the first 12 samples only small changes on the reaction conditions were done. These reactions were only preformed to make a large quantity of functionalized graphene. Since this reaction has only been performed once before by master student Sigmund Mordal Lucasen,

after making the first samples we explored the progress of the reaction by altering the reaction conditions.

First we attempted to alter the amount of malonate used. The same experimental procedure is maintained i.e. graphene is produced in a tip sonicator where graphite (about 0.05 g) is exfoliated in NMP (about 30 mL) at 63 Watt in an icebath for 30 min. The reaction takes place in either *o*-DCB or NMP through filtration and redispersion of produced exfoliated graphene. Table III contains the variables of this reaction set.

Table III: Different samples of functionalized graphene with different amount of malonate.

Sample	Malonate	Graphene		Figure
	[mL]	mL	Solvent	
KE-GM13	0.1	3.0	<i>o</i> -DCB	
KE-GM14	0.1	3.0	NMP	
KE-GM15	0.05	3.0	NMP	
KE-GM16	0.05	3.0	<i>o</i> -DCB	
KE-GM17	0.025	3.0	<i>o</i> -DCB	
KE-GM18	0.010	3.0	NMP	

Results and discussion

As shown in Table III the amount of malonate used for functionalization was varied. Visual verification of dispersion color showed that the reduction of malonate had little or no effect on the amount of graphene that was functionalized. The difference between sample KE-GM14 and KE-GM15 is that the amount of malonate used (KE-GM15 is half the amount used in KE-GM14). Comparing the color of these two (Fig 2.8) shows no change in color, and it can be assumed that the same amount of graphene is functionalized and that only a small amount of malonate is needed. To see how little that can possibly be used, further testing will be done.

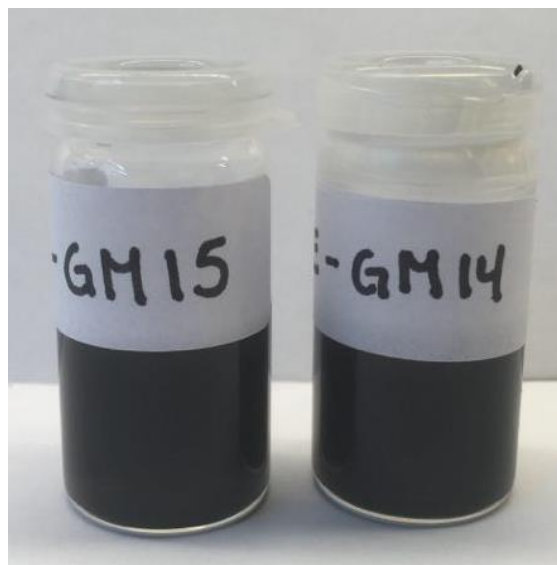


Figure 2.8: Sample KE-GM15 and KE-GM14.

The same test was done using graphene dissolved in *o*-DCB in sample KE-GM16 and KE-GM17. A comparison of KE-GM16 and KE-GM17 is showed in Figure 2.9. There could be observed a slightly lighter color on sample KE-GM17 that can indicate that the amount of malonate was too little, but the difference in color were minimal.

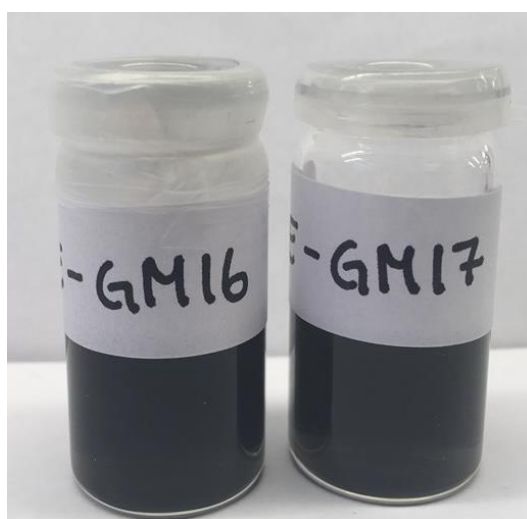


Figure 2.9: Sample KE-GM16 and KE-GM17.

Results and discussion

To see if even smaller amount of malonate can be used, sample KE-GM18 contains only 0,010 mL of malonate. In figure 2.10 this sample is compared to sample KE-GM17 that contains 0,025 mL of malonate. There is no visible difference in the color of the two samples. For further testing the amount of malonate used will be held at 0.010 mL.

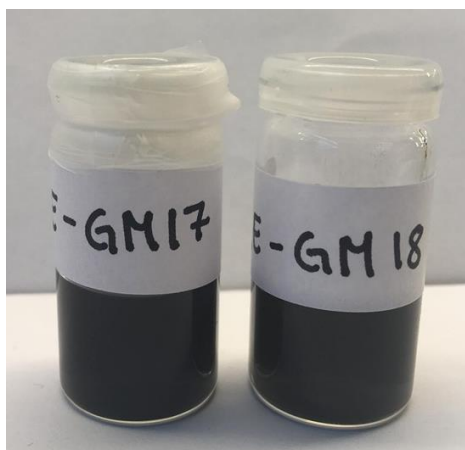


Figure 2.10: Sample KE-GM17 and KE-GM18

Subsequently the amount of the halogen source can be altered. Although both the base (DBU) and CBr_4 are relatively cheap reagents and are typically used in excess, the possibility of needing larger quantities of product through multiple reactions makes the reduction of these reagents a positive development and more environmentally friendly. In Table IV samples with different amount of CBr_4 used to functionalize the graphene is presented. As the figures shows there is no visible difference between using about 0,5 g of CBr_4 and about 0,1 g. The amount of DBU were also attempted to be reduced from 0,4 mL to 0,05 mL, and the results is shown in Table V. The samples that were tested with different amount of DBU had different reaction time in the microwave (20 and 30 minutes), but the sample with the smallest amount of DBU had the shortest reaction time and as there were no difference in color, the amount of DBU was presumed to be sufficient. For further testing the amount of CBr_4 will be around 0,1 g and the amount of DBU around 0,05 mL.

Table IV: Samples of functionalized graphene using different amount of CBr₄.

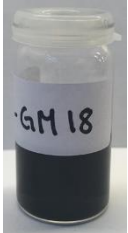

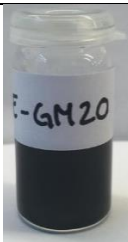
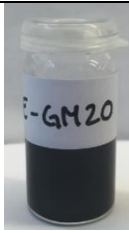
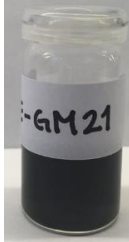
Sample	CBr ₄	Figure
KE-GM18	0,5372	
KE-GM19	0,2459	
KE-GM20	0,1222	

Table V: Samples of functionalized graphene with different amount of DBU.

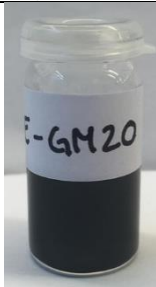
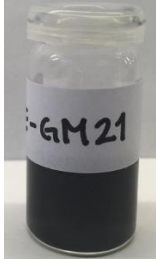

Sample	DBU [mL]	Figure
KE-GM20	0,4	
KE-GM21	0,05	

All the testing that have been done this far has showed great potential. The amount of malonate, CBr₄ and DBU have been reduced successfully. The aim is to optimize the functionalization even more and to make the process more efficient the reaction time in the microwave was

Results and discussion

reduced. Table VI shows different samples that are prepared in the exact same way except the reaction time in the microwave. All the other parameters are listed in Table IX in the appendix. Figure 2.11 compares the color of the samples with different reaction time, and it shows no difference using 30, 20 or 10 minutes.

Table VI: Samples of functionalized graphene with different reaction time in the microwave.

Sample	Time [min]	Figure
KE-GM20	30	
KE-GM21	20	
KE-GM22	10	

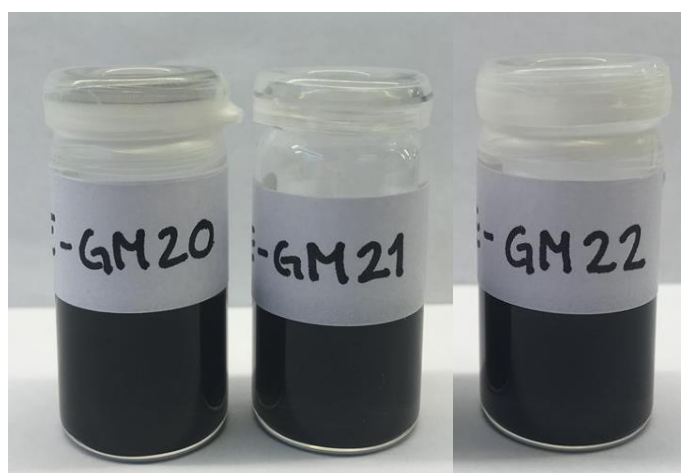


Figure 2.11: Sample KE-GM20, 21 and 22 with different reaction time in the microwave.

After testing different reaction times where it seemed to yield the same results using 10 minutes and 30 minutes, the change of temperature was tested. In Figure 2.12 sample KE-GM22 has been obtained at 120 °C for 10 minutes while sample KE-GM23 has been obtained at 90 °C for 10 minutes. As sample KE-GM23 is not as dark as KE-GM22 it shows that there is less functionalized graphene in the solution. This means that the cyclopropanation reaction requires temperatures higher than 90 °C for the functionalization to proceed even under microwave irradiation. After 48 hours sample KE-GM23 had no color and the grey particles had precipitated. This indicates that the grey color is only exfoliated graphene dispersed in DCM, and no/limited functionalization took place.

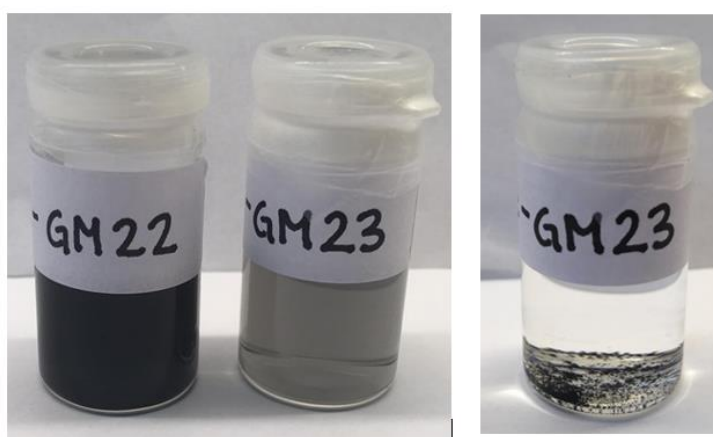


Figure 2.12: (left) Sample KE-GM22 and KE-GM23 obtained at respectively 120 °C and 90 °C.
(right) Sample KE-GM23 after 48 hours.

One other parameter that can be changed on the microwave is the power. All the samples above have been obtained at 40 Watt. Sample KE-GM24 was obtained at 30 Watt. In this sample the amount of graphene that was functionalized was small, as can be seen based on the light grey color of the sample (Fig 2.13). In KE-GM26 the reaction time was increased from 10 minutes to 20 minutes. The color on sample KE-GM26 is a lot darker than the color of KE-GM24. This shows that there exists some balance between microwave intensity and reaction time. However, even if the reaction time was longer, the amount of functionalized graphene was not as much as what was obtained at 40 Watt for 10 minutes.

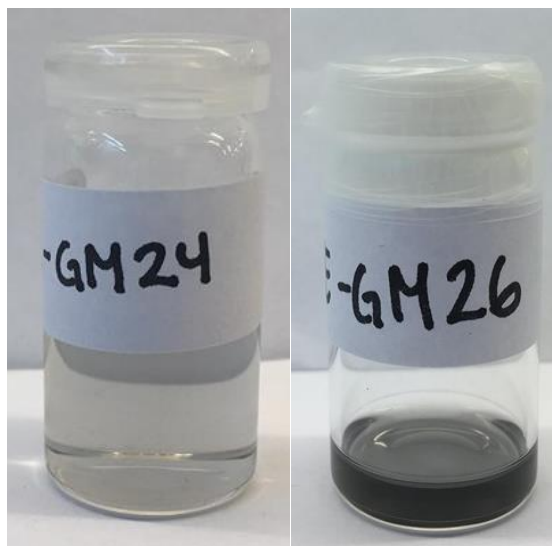




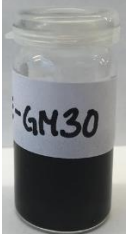
Figure 2.13: Sample KE-GM24 obtained at 30 Watt for 10 minutes and KE-GM26 obtained at 30 Watt for 20 minutes.

After the required amount of functionalized graphene was made some more experimenting was done. Making more functionalized graphene in the same reaction was tested even if this has shown to have some limitations. The quantity of exfoliated graphene that is used in the reaction is not measurable, and the concentration of graphene cannot be too high before it aggregates in NMP,³³ and the microwave doesn't allow for larger vials than 20 mL. Economopoulos *et al.*³⁹ tried upscaling similar reactions, but black dispersions were not obtained. Regardless, we tried to use a larger volume of graphene to explore how the reaction was affected.

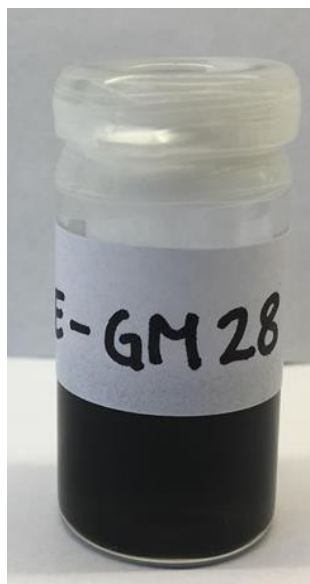
Sample KE-GM25 contains the same amount of malonate, CBr_4 and DBU, and the same setting in the microwave as for example KE-GM22, but the amount of graphene is raised from 3 mL to 5 mL. Sample KE-GM25 is a clear solution and seems to contain no functionalized graphene at all. This result seems to corroborate the results of Economopoulos *et al.*³⁹. If we aim for a larger amount to be functionalized, a longer reaction time or more malonate might be needed.

In sample KE-GM30 the amount of all reagents was increased, and the reaction time was increased. The result is shown in Table VII, and the result is a dark dispersion with no visible differences between KE-GM22 and KE-GM30. It seems to be successful, but to be sure that the functionalization was successful both microRAMAN and TGA must be done.

Table VII: Functionalization of different amounts of graphene.

	KE-GM22	KE-GM25	KE-GM30
Graphene	3,0	5,0	9,0
Malonate	0,01	0,01	0,03
CBr₄	0,0753	0,0671	0,2154
DBU	0,05	0,05	0,20
Figure			

During all the samples above, the microwave has had a pressure at 5 bar, and cooling have been on. As shown in Figure 2.14, a large amount of graphene was functionalized without cooling. There has been no visible change in the color after five days and it can be assumed that the cooling in the microwave might not be necessary. The difference is that when the cooling is on, the power and subsequently the temperature curves are smoother compared to no cooling (Fig 2.15).

**Figure 2.14:** Sample KE-GM28 obtained without cooling in the microwave.

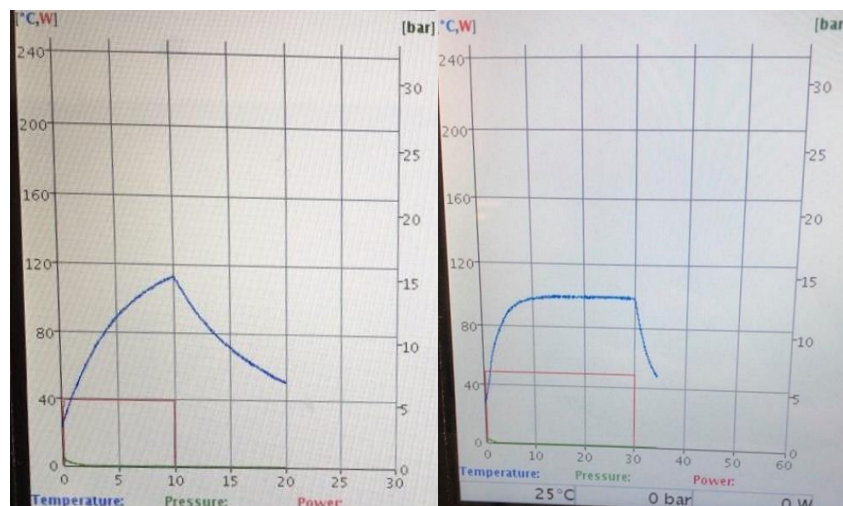


Figure 2.15: The graph from the microwave while obtaining sample KE-GM28 and KE-GM4

Summarizing all the reactions that have been attempted in this project there has been a lot of successful outcomes. Samples KE-GM1 – KE-GM-13 (Figure 2.16) were all obtained in roughly the same way. These were made to fulfill the required amount of product for the research project in order to test these in a MMM for use in capturing CO₂. The master theseis aimed to synthesize two additional ethylene glycol-containing oligomers with different anchoring groups to be tested in other than cyclopropanation (Bingel) reaction pathways. When this was impossible to implement due to the lock-down, this project was changed to optimizing the process for simpler and more efficient production in the future.

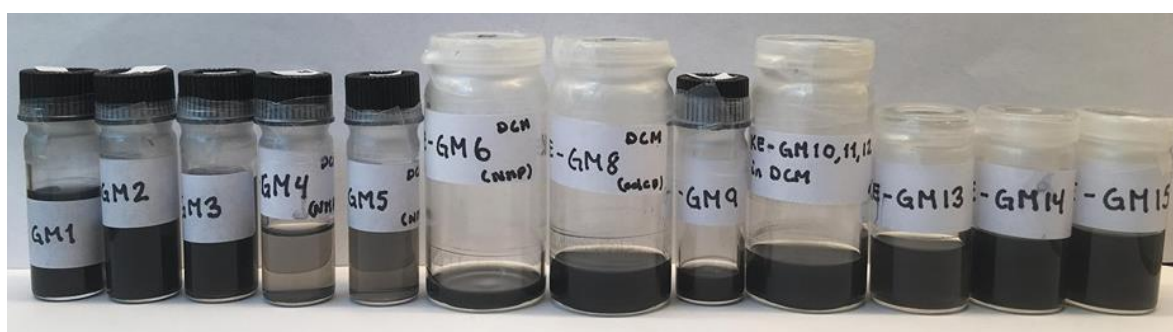


Figure 2.16: Samples KE-GM1 through KE-GM515 of functionalized graphene.

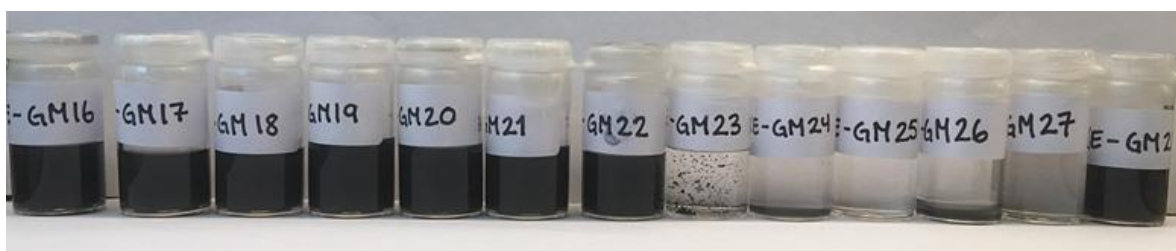


Figure 2.17: Samples KE-GM16 through KE-GM28 of functionalized graphene.

All the samples from KE-GM13 – KE-GM30 (Fig 2.16 and 2.17) have been obtained with the aim to optimize the process and changes in each sample have been observed. The results obtained from all this testing has shown that the cyclopropanation reaction is very tolerant to reaction conditions and the production of functionalized graphene is facilitated. This project outlined the most efficient ways, and based on visual inspection it seems like sample KE-GM22 can offer comparable results as the ones obtained with a larger amount of malonate and with a longer reaction times. This sample is obtained using a very small amount of malonate and with only 10 minutes reaction time. Reducing temperature or power leads to reduced quantities of product. Sample KE-GM30 showed promising results regarding upscaling of the reaction.

Finally, a test was done to check the solubility of the functionalized graphene in different solvents. The functionalized graphene must be dispersible in a solvent to be able to be used in i.e a MMM. Three different samples, KE-GM15, KE-GM16 and KE-GM17 had their solubility tested in solvents with varying polarity and physicochemical properties such as hexane, ethyl acetate, petroleum ether, DMF and water. The results are summarized in Table VIII and shows that the functionalized graphene is most dispersible in DCM.

Table VIII: Solubility of sample KE-GM15, 16 and 17 in hexane, ethyl acetate, petroleum ether, DMF and water.

	KE-GM15	KE-GM16	KE-GM17
DCM	yes	yes	yes
Hexane	no	no	no
Ethyl acetate	partly	partly	partly
Petroleum ether	no	no	no
DMF	partly	partly	partly
Water	no	no	no

3. Conclusion

Graphene was successfully functionalized using microwave assisted Bingel reaction conditions. Graphene was produced in sufficient quantities through exfoliation of graphite using a tip sonicator. 2-(2-(2-Ethoxyethoxy)ethoxy)ethylethylmalonate was successfully synthesized following synthetic protocols developed in-house. The aim of this project was to make a large quantity of functionalized graphene and to optimize the functionalization procedure. Changing the different parameters in the reaction afforded positive results, but the most efficient was sample KE-GM22. KE-GM22 was obtained using graphene made from graphite in NMP sonicated at 63 W for 30 minutes while placed in an icebath. Exfoliated graphene (3 ml) was then reacted with 0,075 g of CBr₄, 0,01 mL of malonate and 0,05 mL of DBU. This was irradiated in the microwave for 10 minutes at 120 °C, 40 Watts, under air cooling. These conditions seemed to obtain good functionalization, with shortened reaction times and efficient reagent usage. Upscaling this reaction was attempted (KE-GM30) and seemed to be efficient using more time in the microwave. Spectroscopic characterization of produced hybrids was carried out using microRAMAN, verifying the covalent attachment of the hybrid while physicochemical verification was obtained by solubility testing in common organic and aqueous solvents, which promote aggregation on unfunctionalized graphene dispersions. Conclusion of the characterization for graphene derivatives requires the quantification of the organic addends per number of carbon atoms of graphitic backbone which was scheduled to be carried out using thermogravimetric analysis (TGA). However, as the instrumentation is located at the Dept of Material Science and requires training and has a long queue of users, time constraints have not permitted the inclusion of these results. Full characterization will take place at the National Energy Technology Laboratory (NETL) at the USA and results will be published.

Acknowledgements

The research Council of Norway is acknowledged for the support to the Norwegian Micro- and Nano – Fabrication Facility, NorFab, project number 245963/F50.

4. Future work

To be able to overcome the environmental challenges the world is facing today due to the large emission of CO₂, carbon capture and storage is of great importance. Developing new strategies for capturing CO₂ potentially has a large impact on the earth and its future. Research in this field is therefore essential, and there is a lot of unexplored areas to examine.

The aim of this project originally was to implement the 2-(2-(2-ethoxyethoxy)ethoxy)ethylethylmalonate – functionalized graphene into a MMM for use in carbon capture. Since this was delayed due to world-wide lockdown, this project was focused on the optimization of the functionalization procedure, and no testing for use in carbon capture was done. Future work includes more microRAMAN testing of various samples to obtain spectroscopic data alongside visual confirmation. More importantly thermogravimetric analysis must be done to quantify the actual number of 2-(2-(2-ethoxyethoxy)ethoxy)ethylethylmalonate groups anchored onto graphene. Finally, the actual implementation of the 2-(2-(2-ethoxyethoxy)ethoxy)ethylethylmalonate – functionalized graphene into a MMM and its performance in CO₂-capture is already scheduled.

It can be useful to explore different routes to functionalize graphene with the malonate and do TGA and microRAMAN analyses to compare the different routes. In addition to testing this exact type of functionalized graphene, it will be important to find other groups to functionalize on to graphene for use in MMMs. One suggestion is to attach 4-(2-aminoethyl)aniline onto graphene. Initial attempts have been made as part of this project, but the functionalization was not successful, and there was no time for additional optimizations.

5. Experimental

5.1 Preparation of 2-(2-(2-ethoxyethoxy)ethoxy)ethylethylmalonate

KE-M1:

CH₂Cl₂ (Dry, 50 mL) was cooled down to 0 °C before 2-(2-(2-ethoxyethoxy)ethoxy)ethane-1-ol (1.75 mL, 0.01 mol) and pyridine (1.00 mL, excess) was added. Further ethyl-3-chloro-3-oxopropanoate (1.28 mL, 0.01 mol) was added slowly (1 drop every 10th second). The reaction mixture was left for 1 hour at 0 °C and then the temperature was increased to room temperature. After three days the reaction mixture was washed with brine (5*40 mL), dried over MgSO₄ and CH₂Cl₂ was evaporated under reduced pressure. ¹H-NMR (400 Hz, CDCl₃): δ: 1.23 – 1.19 (t, ³J_{HH} = 6.96, 3H), δ: 1.30 – 1.26 (t, ³J_{HH} = 7.17, 3 H), δ: 3.40 (S, 2 H), δ: 3.55 – 3.50 (q, ³J_{HH} = 6.94, 2 H), δ: 3.73 – 3.58 (m, 10 H), δ: 4.23 – 4.18 (q, ³J_{HH} = 7.02, 2H), δ: 4.32 – 4.29 (t, ³J_{HH} = 4.84, 2 H). Yield: 2.50 g, 0.0086 mol, 86 %

KE-M2:

KE-M2 was made following the same procedure as for KE-M1, but it was washed with distilled water (2*40 mL) in addition to brine. ¹H-NMR (400 Hz, CDCl₃): δ: 1.23 – 1.19 (t, ³J_{HH} = 6.96, 3H), δ: 1.30 – 1.27 (t, ³J_{HH} = 7.17, 3 H), δ: 3.40 (S, 2 H), δ: 3.55 – 3.50 (q, ³J_{HH} = 6.94, 2 H), δ: 3.73 – 3.58 (m, 10 H), δ: 4.23 – 4.18 (q, ³J_{HH} = 7.02, 2H), δ: 4.32 – 4.29 (t, ³J_{HH} = 4.84, 2 H). Yield: 2.77 g, 0.0095 mol, 95 %

KE-M3

KE-M3 was made following the same procedure as for KE-M2. ¹H-NMR (400 Hz, CDCl₃): δ: 1.23 – 1.19 (t, ³J_{HH} = 6.96, 3H), δ: 1.30 – 1.26 (t, ³J_{HH} = 7.10, 3 H), δ: 3.41 (S, 2 H), δ: 3.55 – 3.50 (q, ³J_{HH} = 6.94, 2 H), δ: 3.73 – 3.58 (m, 10 H), δ: 4.23 – 4.18 (q, ³J_{HH} = 7.02, 2H), δ: 4.32 – 4.29 (t, ³J_{HH} = 4.84, 2 H). Yield: 2.56 g, 0.0088 mol, 88 %

KE-M4

KE-M4 was made following the same procedure as for KE-M2 except that the reaction time was reduced by one day due to the lock-down of campus because of COVID-19. ¹H-NMR (400 Hz, CDCl₃): δ: 1.23 – 1.19 (t, ³J_{HH} = 6.96, 3H), δ: 1.30 – 1.26 (t, ³J_{HH} = 7.10, 3 H), δ: 3.41 (S, 2 H), δ: 3.55 – 3.50 (q, ³J_{HH} = 6.94, 2 H), δ: 3.73 – 3.58 (m, 10 H), δ: 4.23 – 4.18 (q, ³J_{HH} = 7.02, 2H), δ: 4.32 – 4.29 (t, ³J_{HH} = 4.84, 2 H). Yield: 2.38 g, 0.0081 mol, 81 %

Experimental

KE-M5

KE-M5 was made following the same procedure as for KE-M2. $^1\text{H-NMR}$ (400 Hz, CDCl_3): δ : 1.23 – 1.19 (t, $^3J_{\text{HH}} = 6.96$, 3H), δ : 1.30 – 1.26 (t, $^3J_{\text{HH}} = 7.10$, 3 H), δ : 3.41 (s, 2 H), δ : 3.55 – 3.50 (q, $^3J_{\text{HH}} = 6.94$, 2 H), δ : 3.73 – 3.58 (m, 10 H), δ : 4.23 – 4.18 (q, $^3J_{\text{HH}} = 7.02$, 2H), δ : 4.32 – 4.29 (t, $^3J_{\text{HH}} = 4.84$, 2 H). Yield: 2.32 g, 0.0079 mol, 79 %

5.2 Preparation of graphene

Graphene was made by sonication of graphite in 1-methyl-2-pyrrolidone (NMP). Graphite (about 500 mg) was dissolved in NMP (about 30 mL) before it was sonicated at 90 % (63 Watt) in a Bandelin SONOPULS HD2070 70W sonicator for 30 minutes while the vial was placed in an icebath (1 L). After sonication the graphene was centrifuged (4000 rpm, 7 min) and redispersed in *o*-DCB or just kept in NMP but the amount of NMP was reduced to make the concentration of graphene higher. This was done filtrating the supernatant through an Omnipore 0,45 μm PTFE membrane and the filtercake was bath sonicated in 9 mL of either NMP or *o*-DCB. This is the standard procedure used for most of the samples. Some of the samples of graphene was prepared using lower wattage, longer time or without icebath. These variations are all listed in Table IX.

5.3 Functionalization of graphene with 2-(2-(2-ethoxyethoxy)ethoxy)ethylethylmalonate 2-(2-(2-ethoxyethoxy)ethoxy)ethylethylmalonate (0,4 – 0,5 mL) was added to CBr_4 (0,4 – 0,6 g), before graphene (2 – 3 mL) and then DBU (0,4 mL) was added under an inert atmosphere. Different amounts of all the reagents were used, and the exact amount is listed in Table IX together with the parameters used in the microwave. After the addition of DBU the reaction mixture was inserted into the microwave. The graphene that is used is dissolved in *o*-DCB or NMP, this is also listed in Table IX.

5.4 Workup of functionalized graphene

After the Bingel reaction by the microwave the reaction mixture is filtered through an Omnipore 0,45 μm PTFE membrane and washed with DMF (100 mL), methanol (100 mL) and DCM (100 mL). The filtercake was then bath sonicated in DCM (5 mL) before the reaction mixture was centrifuged (4000 rpm, 4 min) and the supernatant were transferred into a new vial before the colour of the sample were compared to other samples.

FAILED REACTIONS

5.5 Functionalization of graphene with 4-(2-aminoethyl)aniline

KE-GA1

4-(2-Aminoethyl)aniline (0.0819 g) was added to exfoliated graphene in *o*-DCB (6 mL) and left for stirring at 120 °C. After 96 hours the mixture was filtered through Omnipore 0,45 µm PTFE membrane and washed with *o*-DCB, methanol, and DCM. The product was collected from the top of the filter and re-dispersed in DCM.⁵⁶ After work up, filtering, centrifuging and redispersion, the supernatant was almost completely see-through.

5.6 Characterization techniques

In this chapter the different characterization techniques that has been used in this project will be presented. Various techniques have been used to identify and characterize the substances that have been made. To characterize the malonate mass spectrometry (MS), infrared spectroscopy (IR) and nuclear magnetic resonance spectroscopy (NMR) was used. Raman spectroscopy was used to determine the functionalization of graphene and the quality of the graphene sheets.

Spectroscopy is a term used for some methods for analyses of molecules and atoms by interpreting the spectra of the molecules and atoms. Each element emits or absorbs electromagnetic radiation in a pattern that is characteristic for that exact element. In the following sequences different spectroscopic characterization techniques will be presented.

5.6.1 Infrared spectroscopy

Using infrared spectroscopy (IR) a sample is irradiated with infrared radiation (wavelengths in the range 2×10^{-4} - 1×10^{-6}) and the compound will absorb the frequency of the light that is equal to the vibrational frequency of the compound. There are several different vibration modes of a molecule (Fig 5.6.1), like stretching, scissoring and rocking⁶⁵.

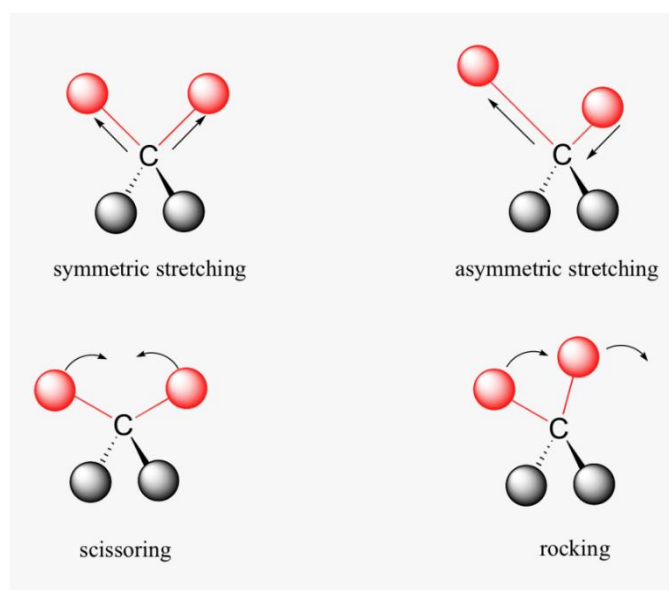


Figure 5.6.1: Different modes of molecular vibration such as stretching, both symmetric and asymmetric, scissoring and rocking.

Measuring the intensity after the irradiation of the compound will give the infrared spectra of the compound. Each compound has its own unique spectrum, like a fingerprint. Different bonds in the molecule will vibrate at different frequencies and therefore many organic groups can easily be identified from the IR-absorption properties ⁶⁵. Considering only the stretching vibrations the vibration frequency gets higher as the bonds between the molecules gets stronger. This means that double bonds vibrate at higher frequency than single bonds, and O-H, N-H and C-H vibrate at higher frequencies than weaker bonds like C-C and C-O.

Historically IR-spectroscopy has been, together with Raman spectroscopy, used to identify the structure of small molecules. These analyses are only partly quantitative and not unambiguous and have therefore often been replaced with NMR and other methods ⁶⁶. In this project IR-spectroscopy have only been used to see if there are any projecting differences in some different samples of functionalized graphene.

5.6.2 Nuclear magnetic resonance spectroscopy

Nuclear magnetic resonance spectroscopy (NMR) is a characterization technique where the nucleus of an atom is observed when placed in a constant magnetic field and electromagnetic radiation is applied. At least one of the isotopes of an atom possess magnetic moments because of spin and the charge of the nucleus, and this isotope behaves like a magnet bar. The spin of an atom is characterized by a quantum number I , and can be $0, \frac{1}{2}, 1, \frac{3}{2}, \dots$. If $I = 0$ there is no

Experimental

spin and no magnetic moment, and $I > \frac{1}{2}$ it has shown to be inconvenient for NMR. NMR is therefore mainly used for nuclei where $I = \frac{1}{2}$. The isotopes that are investigated the most in NMR are ^1H , and ^{13}C which both have $I = \frac{1}{2}$. If a nucleus has spin I , the number of energy states is $2I+1$. This means that a nucleus with spin $I = \frac{1}{2}$ has 2 different energy states and these are referred to as parallel (α) and antiparallel (β), as shown in Figure 5.6.2 where the antiparallel has the highest energy.

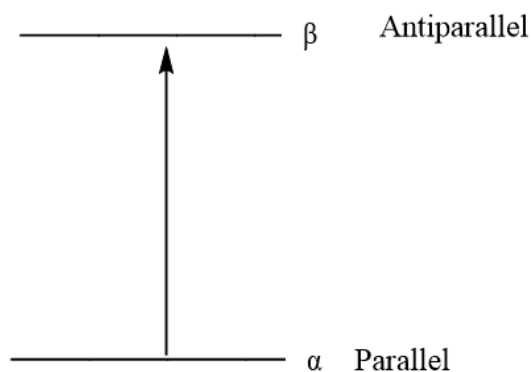


Figure 5.6.2: The two energy states, α and β , of a nucleus with $I = \frac{1}{2}$

Running a NMR the nuclei is exposed to a magnetic field and radiation. The atoms get excited from the lowest energy state (α) to the highest energy state (β) and resonance is obtained. The NMR spectra is generated as the radiation is removed and the atom is returned to its original energy state and energy is emitted. Measurements of the emitted energy and the frequencies where the emission takes place gives information about the nuclei, its surroundings and its stereochemistry. Figure 5.6.3 shows a schematic presentation of a NMR spectrometer. It consists of a magnet, a detector, a transmitter and a computer that prints the signals.

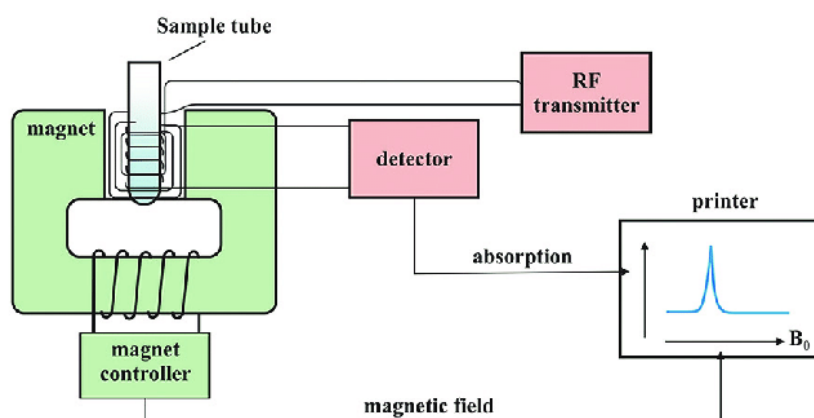


Figure 5.6.3: Schematic presentation of the NMR spectrometer ⁶⁷.

In this project NMR have been used to identify the malonate that was made, and to observe if there were any impurities that needed to be removed before the functionalization of graphene.

5.6.3 Raman spectroscopy

Together with infrared (IR) spectroscopy, Raman spectroscopy is one of the most important characterisation technique in vibrational spectroscopy ⁶⁸. Raman spectroscopy was first introduced by C.V. Raman in 1928 ⁶⁹, and is used to determine different vibration modes which can give a structural fingerprint which makes it possible to identify molecules, and the concentration can also be determined. Often both IR and Raman spectroscopy is necessary to completely measure the vibrational mode of a molecule, because these two techniques are complementary and arises from different processes and selection rules ⁶⁸.

As IR spectroscopy, Raman spectroscopy is based on the different vibrations of the molecule. When the molecule is hit by light it can receive energy from the light and get excited to a higher energy level. When the molecule relaxes back to its original energy level it is called elastic scattering or Rayleigh scattering. In some cases, the molecule relaxes back to a higher or lower energy level than it originally had. This scattering is inelastic and is called Raman scattering, and this is what is measured in Raman spectroscopy. If the molecules go to a higher state than originally it is called Stokes, and if it goes to a lower state it is called anti-stokes (Fig 5.6.4). Measuring the differences in energy in the incoming and outgoing photon, the energy of the molecule can be determined since the energy of the molecule is unique to every molecule and acts as a fingerprint.

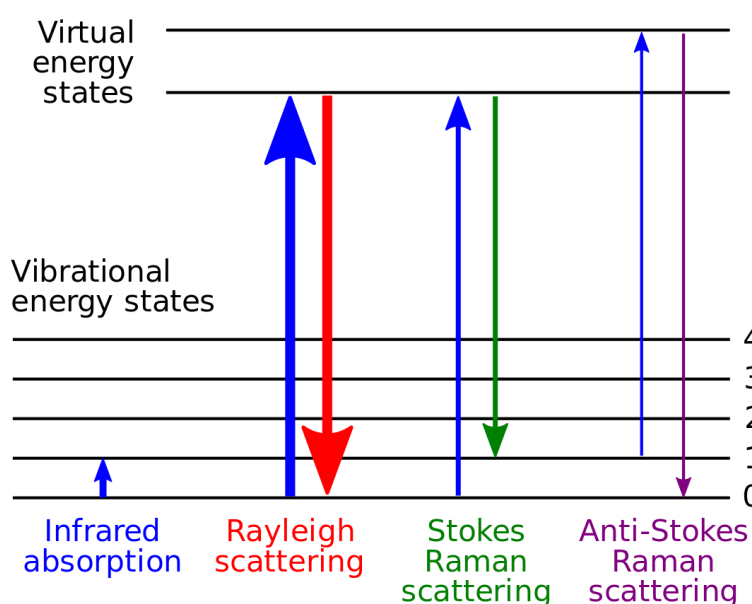


Figure 5.6.4: Different types of scattering when a molecule gets excited and relaxes back.

Experimental

Raman spectroscopy takes place in a Raman spectrometer (Fig 5.6.5). The spectrometer consists of a laser source, a sample illumination system, a suitable spectrometer and a monitoring device. Common laser types are Argon ion, krypton ion, helium-neon and diode. Usually only Stokes scattering is recorded because these are appreciably more intense than the anti-stokes scattering lines.

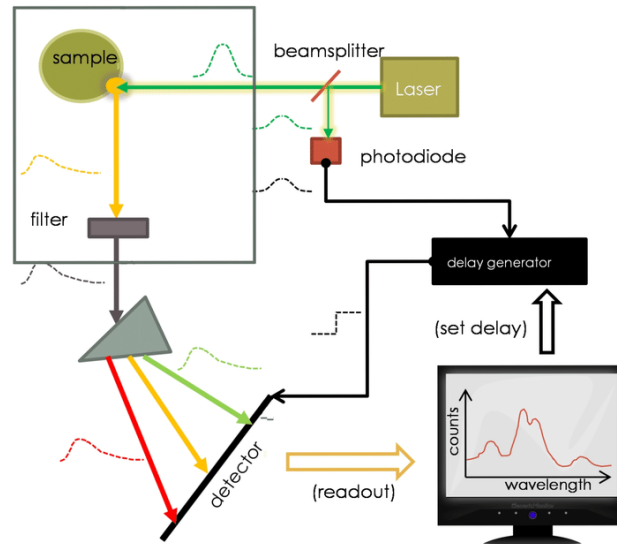


Figure 5.6.5: Schematic presentation of a Raman spectrometer ⁷⁰.

When the Raman scattering have been detected the monitoring-device prints out a Raman spectra. Looking at the energy and patterns of the peaks in the spectra, the structure of the molecule and the pattern of these bands a specific molecule in a sample can be identified.

Raman spectroscopy is of great importance when it comes to graphene and functionalizing graphene. It can both tell something about the quality of the graphene and about how the functionalization. In Figure 5.6.6 the main Raman features of graphene is shown. They are denoted as D, G, D' and G'.

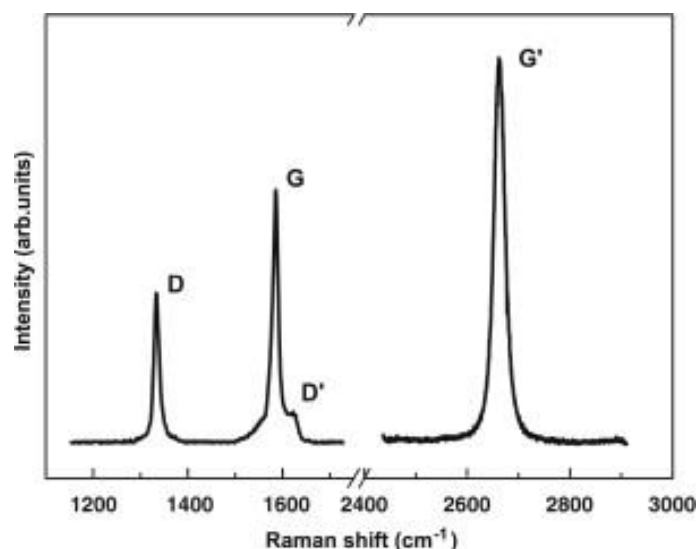


Figure 5.6.6: Raman spectra of the graphene edges, showing the main Raman features the D, D', G and G' bands ⁷¹.

In this project Raman spectroscopy is used to identify the functionalization of graphene.

5.6.4 Mass spectrometry

Mass spectrometry (MS) is an analytical technique that measures the masses of atoms and molecules. This is done in a three-step procedure where the sample first goes through an electron beam and the atoms and molecules are converted into ions since the electrons are knocked out in the electron beam. The positive ions are then passed through an electric field and gets accelerated into a magnetic field. In the magnetic field they get deflected and lighter ions are more deflected than heavier ions. The deflected ions then hit a charged plate that creates a signal that is transferred into a complex diagram which is the mass spectra. The mass spectra show the molecular mass of the ions and the molecules can be both identified and quantified.

5.7 Solubility testing

1 mL of each sample KE-MG15, KE-GM16 and KE-17 was placed in clean vials and allowed for DCM to evaporate. After all the DCM had evaporated, hexane (1 mL) was added to the vials. the precipitate was then bath sonicated in hexane for about 30 seconds before the solution was centrifuged at 2000 rpm for 4 minutes. Visual confirmation of solubility was obtained. The process was repeated for ethyl acetate and petroleum ether. Additionally, separate solubility testing was carried out for DMF and water due to the high boiling point of these solvents.

7. References

1. D'Alessandro, D. M.; Smit, B.; Long, J. R., Carbon Dioxide Capture: Prospects for New Materials. *Angewandte Chemie International Edition* **2010**, *49* (35), 6058-6082.
2. Ahmed, R.; Liu, G.; Yousaf, B.; Abbas, Q.; Ullah, H.; Ali, M. U., Recent advances in carbon-based renewable adsorbent for selective carbon dioxide capture and separation-A review. *Journal of Cleaner Production* **2020**, *242*, 118409.
3. Brunetti, A.; Scura, F.; Barbieri, G.; Drioli, E., Membrane technologies for CO₂ separation. *Journal of Membrane Science* **2010**, *359* (1), 115-125.
4. Sumida, K.; Rogow, D. L.; Mason, J. A.; McDonald, T. M.; Bloch, E. D.; Herm, Z. R.; Bae, T.-H.; Long, J. R., Carbon Dioxide Capture in Metal–Organic Frameworks. *Chemical Reviews* **2012**, *112* (2), 724-781.
5. Jacobson, M. Z., Review of solutions to global warming, air pollution, and energy security. *Energy & Environmental Science* **2009**, *2* (2), 148-173.
6. Jacobson, M. Z., Climate response of fossil fuel and biofuel soot, accounting for soot's feedback to snow and sea ice albedo and emissivity. *Journal of Geophysical Research: Atmospheres* **2004**, *109* (D21).
7. Bains, P.; Psarras, P.; Wilcox, J., CO₂ capture from the industry sector. *Progress in Energy and Combustion Science* **2017**, *63*, 146-172.
8. Change, I. C., The physical science basis. **2007**.
9. Li, B.; Duan, Y.; Luebke, D.; Morreale, B., Advances in CO₂ capture technology: A patent review. *Applied Energy* **2013**, *102*, 1439-1447.
10. Choudhary, P., *Carbon Capture and Storage Program(CCSP) Final report 1.1.2011–31.10.2016*. 2016.
11. Mondal, M. K.; Balsora, H. K.; Varshney, P., Progress and trends in CO₂ capture/separation technologies: A review. *Energy* **2012**, *46* (1), 431-441.
12. Kim, H. W.; Yoon, H. W.; Yoon, S.-M.; Yoo, B. M.; Ahn, B. K.; Cho, Y. H.; Shin, H. J.; Yang, H.; Paik, U.; Kwon, S.; Choi, J.-Y.; Park, H. B., Selective Gas Transport Through Few-Layered Graphene and Graphene Oxide Membranes. *Science* **2013**, *342* (6154), 91-95.
13. Zhao, G. J. M., Membrane Separation Technology in Carbon Capture, Recent Advances in Carbon Capture and Storage. Yun, Y., Ed. IntechOpen: 2017.
14. Balasubramanian, R.; Chowdhury, S., Recent advances and progress in the development of graphene-based adsorbents for CO₂ capture. *Journal of Materials Chemistry A* **2015**, *3* (44), 21968-21989.
15. Malekian, F.; Ghafourian, H.; Zare, K.; Sharif, A. A.; Zamani, Y., Recent progress in gas separation using functionalized graphene nanopores and nanoporous graphene oxide membranes. *The European Physical Journal Plus* **2019**, *134* (5), 212.
16. He, G.; Huang, S.; Villalobos, L. F.; Zhao, J.; Mensi, M.; Oveisi, E.; Rezaei, M.; Agrawal, K. V., High-permeance polymer-functionalized single-layer graphene membranes that surpass the postcombustion carbon capture target. *Energy & Environmental Science* **2019**, *12* (11), 3305-3312.
17. Li, X.; Cheng, Y.; Zhang, H.; Wang, S.; Jiang, Z.; Guo, R.; Wu, H., Efficient CO₂ Capture by Functionalized Graphene Oxide Nanosheets as Fillers To Fabricate Multi-Permselective Mixed Matrix Membranes. *ACS Applied Materials & Interfaces* **2015**, *7* (9), 5528-5537.
18. De Angelis, M. G., Solubility-Selective Membrane. In *Encyclopedia of Membranes*, Drioli, E.; Giorno, L., Eds. Springer Berlin Heidelberg: Berlin, Heidelberg, 2015; pp 1-2.
19. Zuhairun, A. K.; Ismail, A. F., The role of layered silicate loadings and their dispersion states on the gas separation performance of mixed matrix membrane. *Journal of Membrane Science* **2014**, *468*, 20-30.

References

20. Rahman, M. M.; Filiz, V.; Shishatskiy, S.; Abetz, C.; Neumann, S.; Bolmer, S.; Khan, M. M.; Abetz, V., PEBAX® with PEG functionalized POSS as nanocomposite membranes for CO₂ separation. *Journal of Membrane Science* **2013**, *437*, 286-297.
21. Zhao, S.; Wang, Z.; Qiao, Z.; Wei, X.; Zhang, C.; Wang, J.; Wang, S., Gas separation membrane with CO₂-facilitated transport highway constructed from amino carrier containing nanorods and macromolecules. *Journal of Materials Chemistry A* **2013**, *1* (2), 246-249.
22. Dai, Y.; Ruan, X.; Yan, Z.; Yang, K.; Yu, M.; Li, H.; Zhao, W.; He, G., Imidazole functionalized graphene oxide/PEBAX mixed matrix membranes for efficient CO₂ capture. *Separation and Purification Technology* **2016**, *166*, 171-180.
23. Zahri, K.; Goh, P. S.; Ismail, A. F., The incorporation of graphene oxide into polysulfone mixed matrix membrane for CO₂/CH₄ separation. *IOP Conference Series: Earth and Environmental Science* **2016**, *36*, 012007.
24. Pazani, F.; Aroujalian, A., Enhanced CO₂-selective behavior of Pebax-1657: A comparative study between the influence of graphene-based fillers. *Polymer Testing* **2020**, *81*, 106264.
25. Robeson, L. M., Correlation of separation factor versus permeability for polymeric membranes. *Journal of Membrane Science* **1991**, *62* (2), 165-185.
26. Robeson, L. M., The upper bound revisited. *Journal of Membrane Science* **2008**, *320* (1), 390-400.
27. Panapitiya, N.; Wijenayake, S.; Nguyen, D.; Karunaweera, C.; Huang, Y.; Balkus, K.; Musselman, I.; Ferraris, J., Compatibilized Immiscible Polymer Blends for Gas Separations. *Materials* **2016**, *9*, 643.
28. Huang, T.-C.; Liu, Y.-C.; Lin, G.-S.; Lin, C.-H.; Liu, W.-R.; Tung, K.-L., Fabrication of pebax-1657-based mixed-matrix membranes incorporating N-doped few-layer graphene for carbon dioxide capture enhancement. *Journal of Membrane Science* **2020**, *602*, 117946.
29. Zhang, X.; Browne, W.; Wees, B.; Feringa, B., Preparation of Graphene by Solvent Dispersion Methods and Its Functionalization through Noncovalent and Covalent Approaches. 2018; pp 187-203.
30. Taheri Najafabadi, A., Emerging applications of graphene and its derivatives in carbon capture and conversion: Current status and future prospects. *Renewable and Sustainable Energy Reviews* **2015**, *41*, 1515-1545.
31. Novoselov, K. S.; Geim, A. K.; Morozov, S. V.; Jiang, D.; Zhang, Y.; Dubonos, S. V.; Grigorieva, I. V.; Firsov, A. A., Electric Field Effect in Atomically Thin Carbon Films. *Science* **2004**, *306* (5696), 666-669.
32. Parvez, K.; Yang, S.; Feng, X.; Müllen, K., Exfoliation of graphene via wet chemical routes. *Synthetic Metals* **2015**, *210*, 123-132.
33. Hernandez, Y.; Nicolosi, V.; Lotya, M.; Blighe, F. M.; Sun, Z.; De, S.; McGovern, I. T.; Holland, B.; Byrne, M.; Gun'Ko, Y. K.; Boland, J. J.; Niraj, P.; Duesberg, G.; Krishnamurthy, S.; Goodhue, R.; Hutchison, J.; Scardaci, V.; Ferrari, A. C.; Coleman, J. N., High-yield production of graphene by liquid-phase exfoliation of graphite. *Nature Nanotechnology* **2008**, *3* (9), 563-568.
34. Hamilton, C. E.; Lomeda, J. R.; Sun, Z.; Tour, J. M.; Barron, A. R., High-Yield Organic Dispersions of Unfunctionalized Graphene. *Nano Letters* **2009**, *9* (10), 3460-3462.
35. Bourlinos, A. B.; Georgakilas, V.; Zboril, R.; Steriotis, T. A.; Stubos, A. K., Liquid-Phase Exfoliation of Graphite Towards Solubilized Graphenes. *Small* **2009**, *5* (16), 1841-1845.
36. Yang, Q.; Pan, X.; Clarke, K.; Li, K., Covalent Functionalization of Graphene with Polysaccharides. *Industrial & Engineering Chemistry Research* **2012**, *51* (1), 310-317.
37. Singh, R. K.; Kumar, R.; Singh, D. P., Graphene oxide: strategies for synthesis, reduction and frontier applications. *RSC Advances* **2016**, *6* (69), 64993-65011.

References

38. Wang, S.; Zhang, Y.; Abidi, N.; Cabrales, L., Wettability and Surface Free Energy of Graphene Films. *Langmuir* **2009**, *25* (18), 11078-11081.
39. Economopoulos, S. P.; Rotas, G.; Miyata, Y.; Shinohara, H.; Tagmatarchis, N., Exfoliation and Chemical Modification Using Microwave Irradiation Affording Highly Functionalized Graphene. *ACS Nano* **2010**, *4* (12), 7499-7507.
40. Economopoulos, S. P.; Tagmatarchis, N., Chemical Functionalization of Exfoliated Graphene. *Chemistry – A European Journal* **2013**, *19* (39), 12930-12936.
41. Some, S.; Kim, Y.; Hwang, E.; Yoo, H.; Lee, H., Binol salt as a completely removable graphene surfactant. *Chemical Communications* **2012**, *48* (62), 7732-7734.
42. Koros, W. J., Evolving beyond the thermal age of separation processes: Membranes can lead the way. *AIChE Journal* **2004**, *50* (10), 2326-2334.
43. Georgakilas, V.; Otyepka, M.; Bourlinos, A. B.; Chandra, V.; Kim, N.; Kemp, K. C.; Hobza, P.; Zboril, R.; Kim, K. S., Functionalization of Graphene: Covalent and Non-Covalent Approaches, Derivatives and Applications. *Chemical Reviews* **2012**, *112* (11), 6156-6214.
44. Nandanapalli, K. R.; Mudusu, D.; Lee, S., Functionalization of graphene layers and advancements in device applications. *Carbon* **2019**, *152*, 954-985.
45. Hu, S.; Xie, K.; Zhang, X.; Zhang, S.; Gao, J.; Song, H.; Chen, D., Significantly enhanced capacitance deionization performance by coupling activated carbon with triethyltetramine-functionalized graphene. *Chemical Engineering Journal* **2020**, *384*, 123317.
46. Elias, D. C.; Nair, R. R.; Mohiuddin, T. M. G.; Morozov, S. V.; Blake, P.; Halsall, M. P.; Ferrari, A. C.; Boukhvalov, D. W.; Katsnelson, M. I.; Geim, A. K.; Novoselov, K. S., Control of Graphene's Properties by Reversible Hydrogenation: Evidence for Graphane. *Science* **2009**, *323* (5914), 610-613.
47. Bao, Q.; Hui, K. S.; Duh, J. G., Promoting catalytic ozonation of phenol over graphene through nitrogenation and Co₃O₄ compositing. *Journal of Environmental Sciences* **2016**, *50*, 38-48.
48. Loeblein, M.; Perry, G.; Tsang, S. H.; Xiao, W.; Collard, D.; Coquet, P.; Sakai, Y.; Teo, E. H. T., Three-Dimensional Graphene: A Biocompatible and Biodegradable Scaffold with Enhanced Oxygenation. *Advanced Healthcare Materials* **2016**, *5* (10), 1177-1191.
49. Robinson, J. T.; Burgess, J. S.; Junkermeier, C. E.; Badescu, S. C.; Reinecke, T. L.; Perkins, F. K.; Zalalutdniov, M. K.; Baldwin, J. W.; Culbertson, J. C.; Sheehan, P. E.; Snow, E. S., Properties of Fluorinated Graphene Films. *Nano Letters* **2010**, *10* (8), 3001-3005.
50. Yao, Y.; Gao, J.; Bao, F.; Jiang, S.; Zhang, X.; Ma, R., Covalent functionalization of graphene with polythiophene through a Suzuki coupling reaction. *RSC Advances* **2015**, *5* (53), 42754-42761.
51. Quintana, M.; Spyrou, K.; Grzelczak, M.; Browne, W. R.; Rudolf, P.; Prato, M., Functionalization of Graphene via 1,3-Dipolar Cycloaddition. *ACS Nano* **2010**, *4* (6), 3527-3533.
52. Zhang, X.; Hou, L.; Cnossen, A.; Coleman, A. C.; Ivashenko, O.; Rudolf, P.; van Wees, B. J.; Browne, W. R.; Feringa, B. L., One-Pot Functionalization of Graphene with Porphyrin through Cycloaddition Reactions. *Chemistry – A European Journal* **2011**, *17* (32), 8957-8964.
53. Quintana, M.; Vazquez, E.; Prato, M., Organic Functionalization of Graphene in Dispersions. *Accounts of Chemical Research* **2013**, *46* (1), 138-148.
54. Liu, L.-H.; Yan, M., Functionalization of pristine graphene with perfluorophenyl azides. *Journal of Materials Chemistry* **2011**, *21* (10), 3273-3276.
55. Castelaín, M.; Martínez, G.; Merino, P.; Martín-Gago, J. Á.; Segura, J. L.; Ellis, G.; Salavagione, H. J., Graphene Functionalisation with a Conjugated Poly(fluorene) by Click Coupling: Striking Electronic Properties in Solution. *Chemistry – A European Journal* **2012**, *18* (16), 4965-4973.

References

56. Karousis, N.; Ortiz, J.; Ohkubo, K.; Hasobe, T.; Fukuzumi, S.; Sastre-Santos, Á.; Tagmatarchis, N., Zinc Phthalocyanine–Graphene Hybrid Material for Energy Conversion: Synthesis, Characterization, Photophysics, and Photoelectrochemical Cell Preparation. *The Journal of Physical Chemistry C* **2012**, *116* (38), 20564-20573.
57. Bekyarova, E.; Itkis, M. E.; Ramesh, P.; Berger, C.; Sprinkle, M.; de Heer, W. A.; Haddon, R. C., Chemical Modification of Epitaxial Graphene: Spontaneous Grafting of Aryl Groups. *Journal of the American Chemical Society* **2009**, *131* (4), 1336-1337.
58. Sun, Z.; Kohama, S.-i.; Zhang, Z.; Lomeda, J. R.; Tour, J. M., Soluble graphene through edge-selective functionalization. *Nano Research* **2010**, *3* (2), 117-125.
59. Jin, Z.; McNicholas, T. P.; Shih, C.-J.; Wang, Q. H.; Paulus, G. L. C.; Hilmer, A. J.; Shimizu, S.; Strano, M. S., Click Chemistry on Solution-Dispersed Graphene and Monolayer CVD Graphene. *Chemistry of Materials* **2011**, *23* (14), 3362-3370.
60. Bingel, C., Cyclopropanierung von Fullerenen. *Chemische Berichte* **1993**, *126* (8), 1957-1959.
61. Economopoulos, S. P.; Pagona, G.; Yudasaka, M.; Iijima, S.; Tagmatarchis, N., Solvent-free microwave-assisted Bingel reaction in carbon nanohorns. *Journal of Materials Chemistry* **2009**, *19* (39), 7326-7331.
62. Umeyama, T.; Tezuka, N.; Fujita, M.; Matano, Y.; Takeda, N.; Murakoshi, K.; Yoshida, K.; Isoda, S.; Imahori, H., Retention of Intrinsic Electronic Properties of Soluble Single-Walled Carbon Nanotubes after a Significant Degree of Sidewall Functionalization by the Bingel Reaction. *The Journal of Physical Chemistry C* **2007**, *111* (27), 9734-9741.
63. Lucasen, S. M. NTNU, Trondheim, 2020.
64. Trinh, T. M. N.; Holler, M.; Schneider, J. P.; Garcia-Moreno, M. I.; Garcia Fernandez, J. M.; Bodlenner, A.; Compain, P.; Ortiz Mellet, C.; Nierengarten, J.-F., Construction of giant glycosidase inhibitors from iminosugar-substituted fullerene macromonomers. *J. Mater. Chem. B* **2017**, *5* (32), 6546-6556.
65. Cranwell, P. B.; Harwood, L. M.; Moody, C. J., *Experimental organic chemistry*. John Wiley & Sons: 2017.
66. Wibetoe, G. IR-spektroskopi. (accessed 25.05).
67. Zia, K.; Siddiqui, T.; Ali, S.; Farooq, I.; Zafar, M. S.; Sultan, Z., Nuclear Magnetic Resonance Spectroscopy for Medical and Dental Applications: A Comprehensive Review. *European journal of dentistry* **2019**, *13*, 124-128.
68. Larkin, P., Chapter 1 - Introduction: Infrared and Raman Spectroscopy. In *Infrared and Raman Spectroscopy*, Larkin, P., Ed. Elsevier: Oxford, 2011; pp 1-5.
69. Raman, C. V.; Krishnan, K. S., A New Type of Secondary Radiation. *Nature* **1928**, *121* (3048), 501-502.
70. Takalo, J.; Siltanen, S.; Lassas, M.; Rantala, M.; Timonen, J.; Kurki, L., Separating counterfeit and genuine euro banknotes using time-resolved Raman spectroscopy. **2015**.
71. Malard, L. M.; Pimenta, M. A.; Dresselhaus, G.; Dresselhaus, M. S., Raman spectroscopy in graphene. *Physics Reports* **2009**, *473* (5), 51-87.

8. Appendix

8.1 NMR – spectra of 2-(2-(2-ethoxyethoxy)ethoxy)ethylmalonate

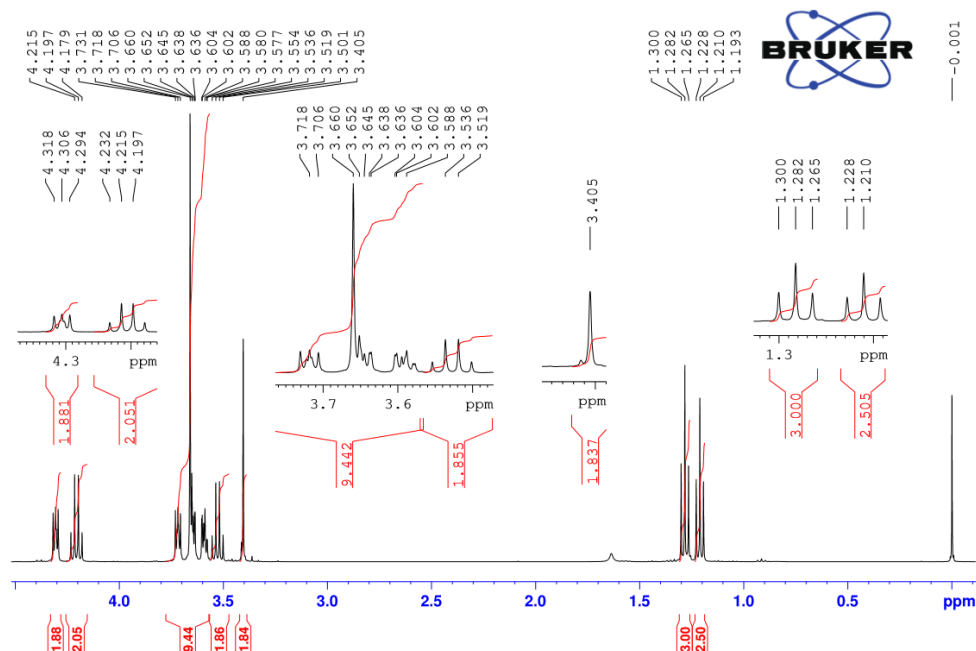


Figure 8.1.1: ¹H-NMR spectra for sample KE-M1.

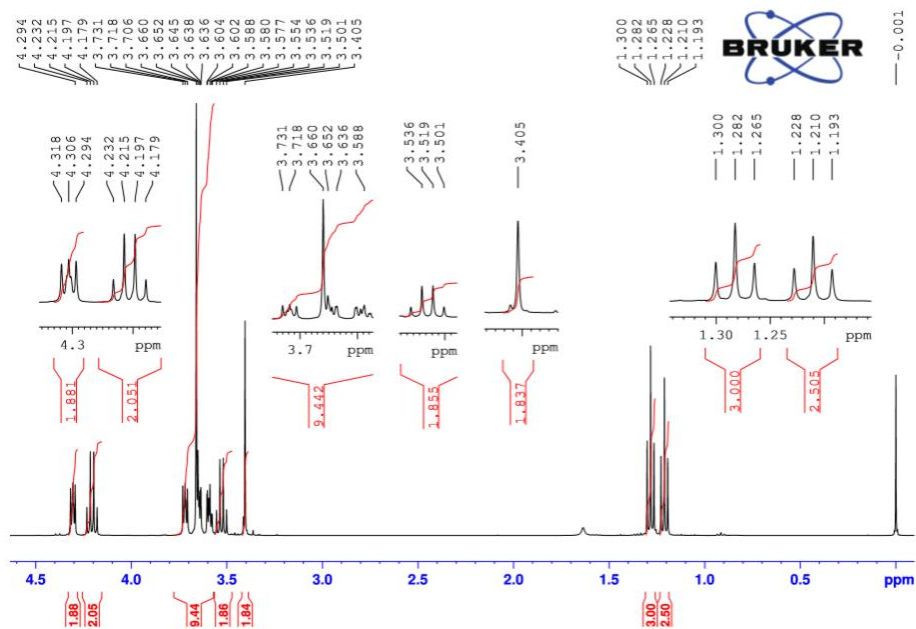


Figure 8.1.2: ¹H-NMR spectra for sample KE-M2.

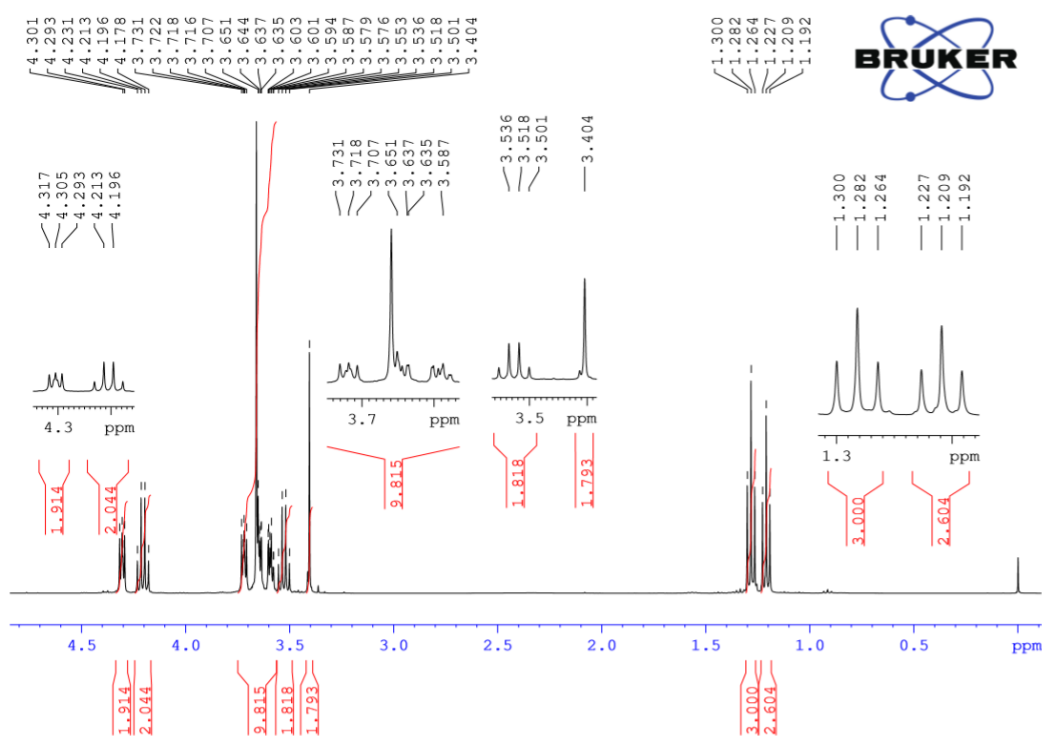


Figure 8.1.3: ¹H-NMR spectra for sample KE-M3.

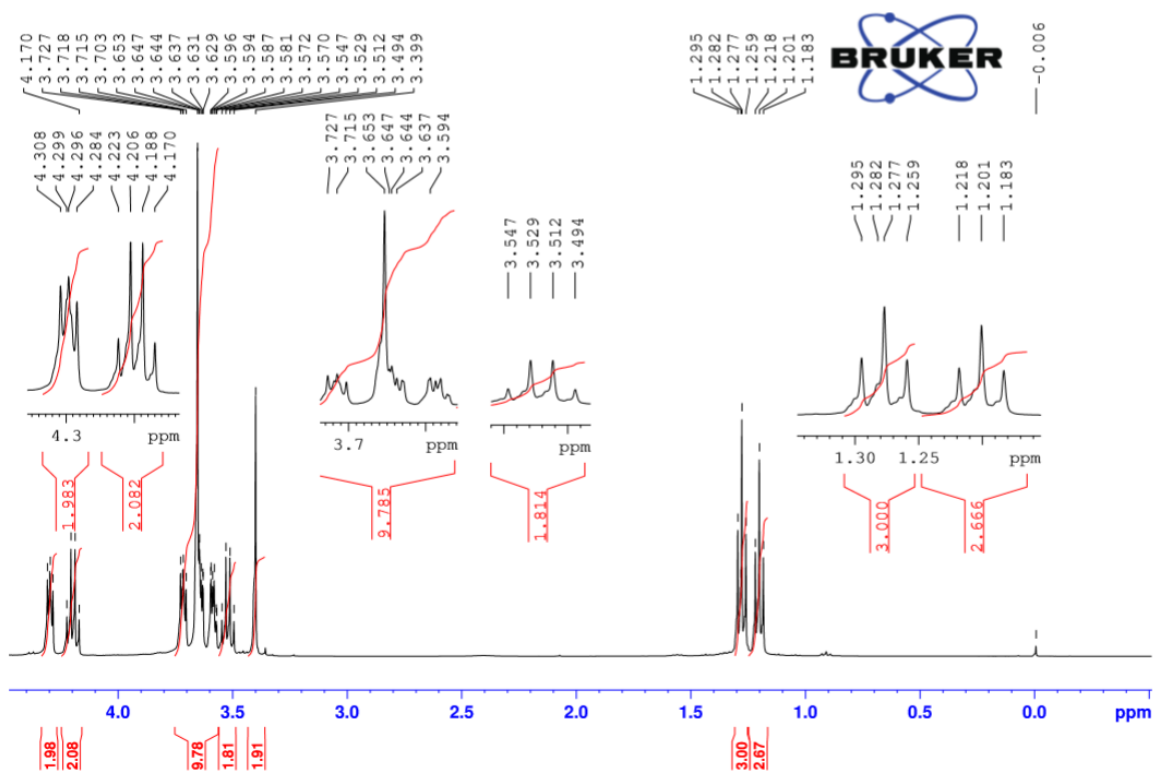


Figure 8.1.4: ¹H-NMR spectra for sample KE-M4

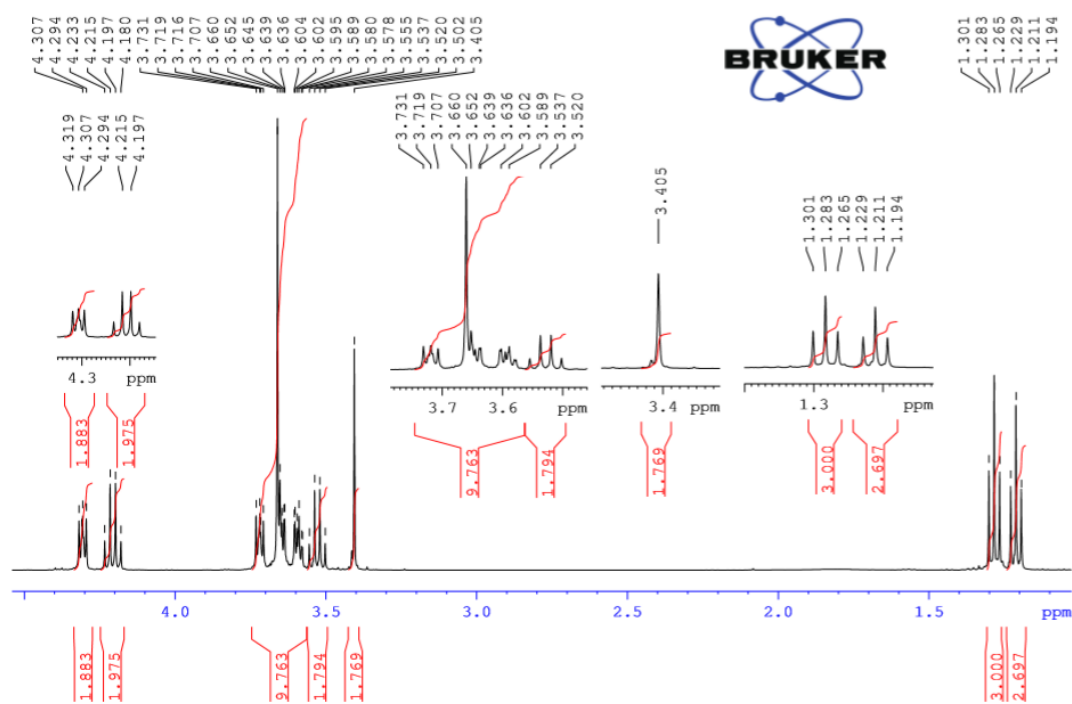


Figure 8.1.5: ¹H-NMR spectra for sample KE-M5

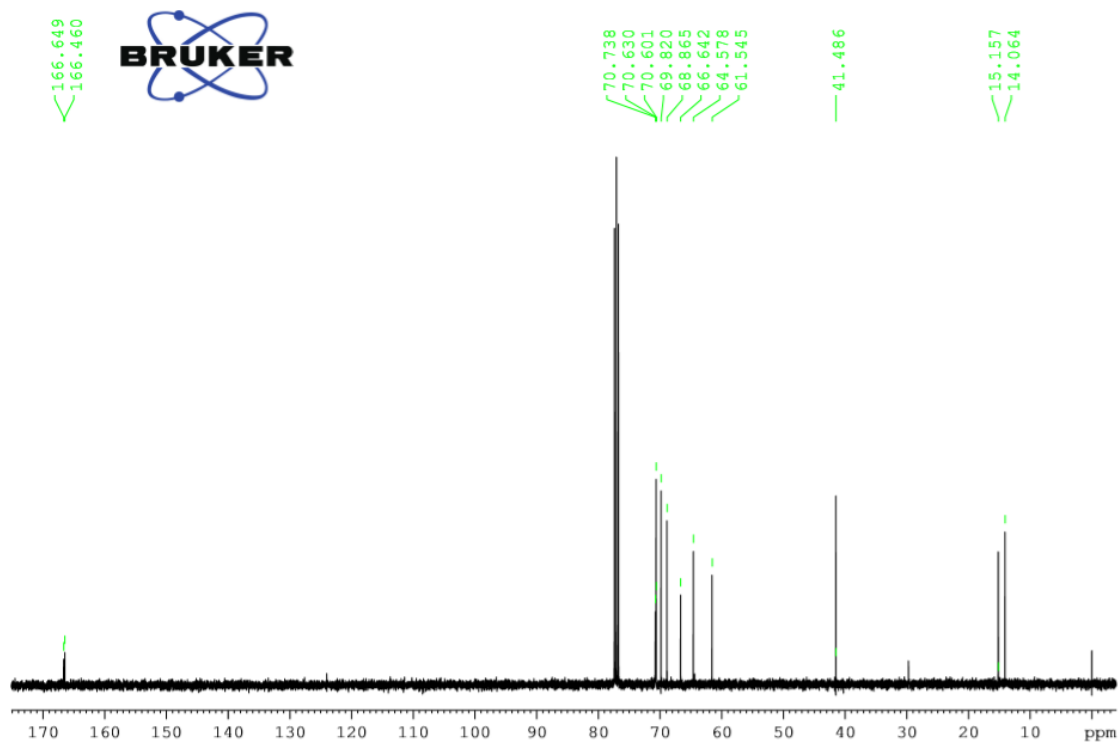


Figure 8.1.6: ¹³C-NMR spectra for sample KE-M5.

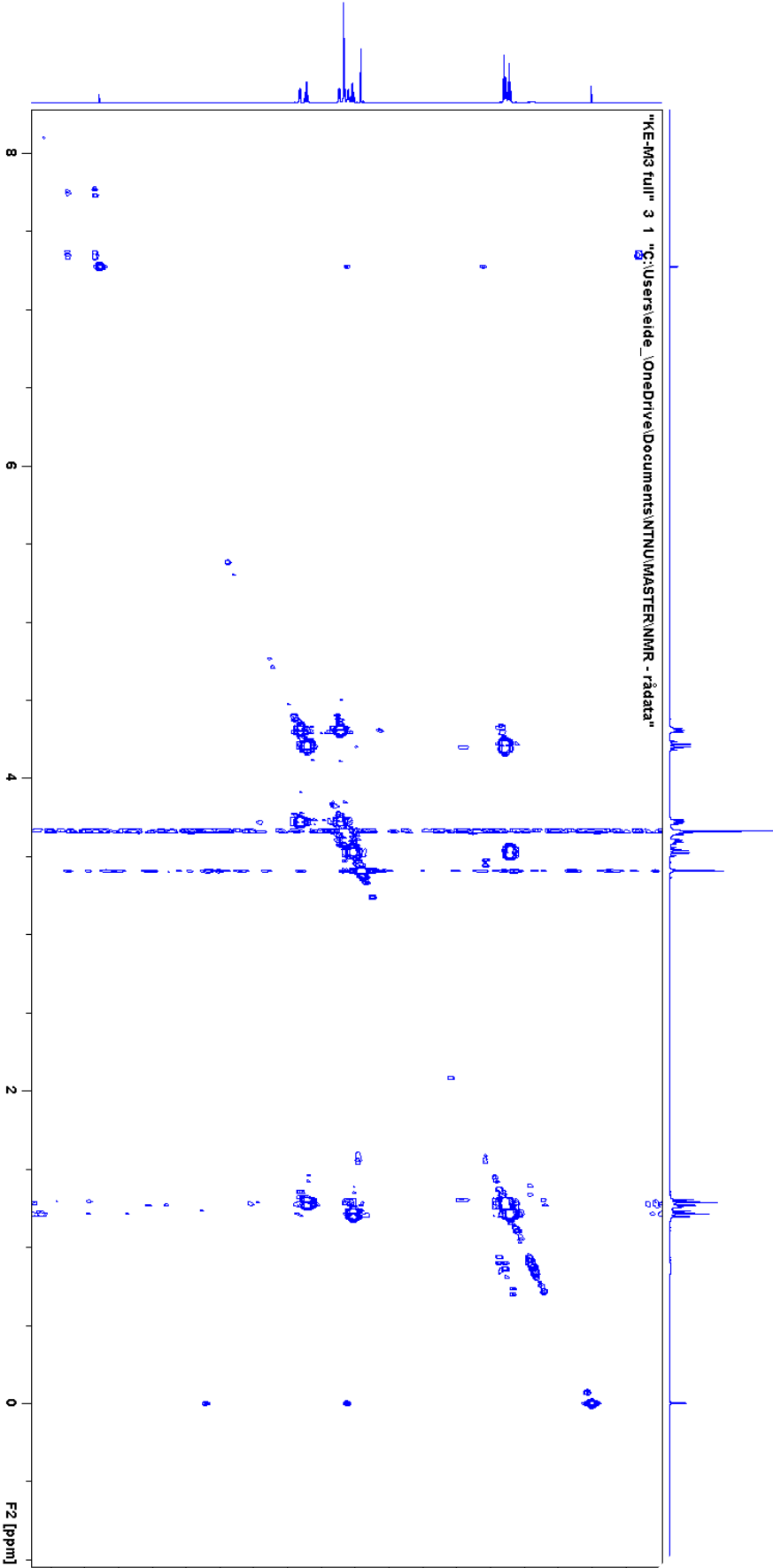


Figure 8.1.7: C cosy-spectra of KE-M3

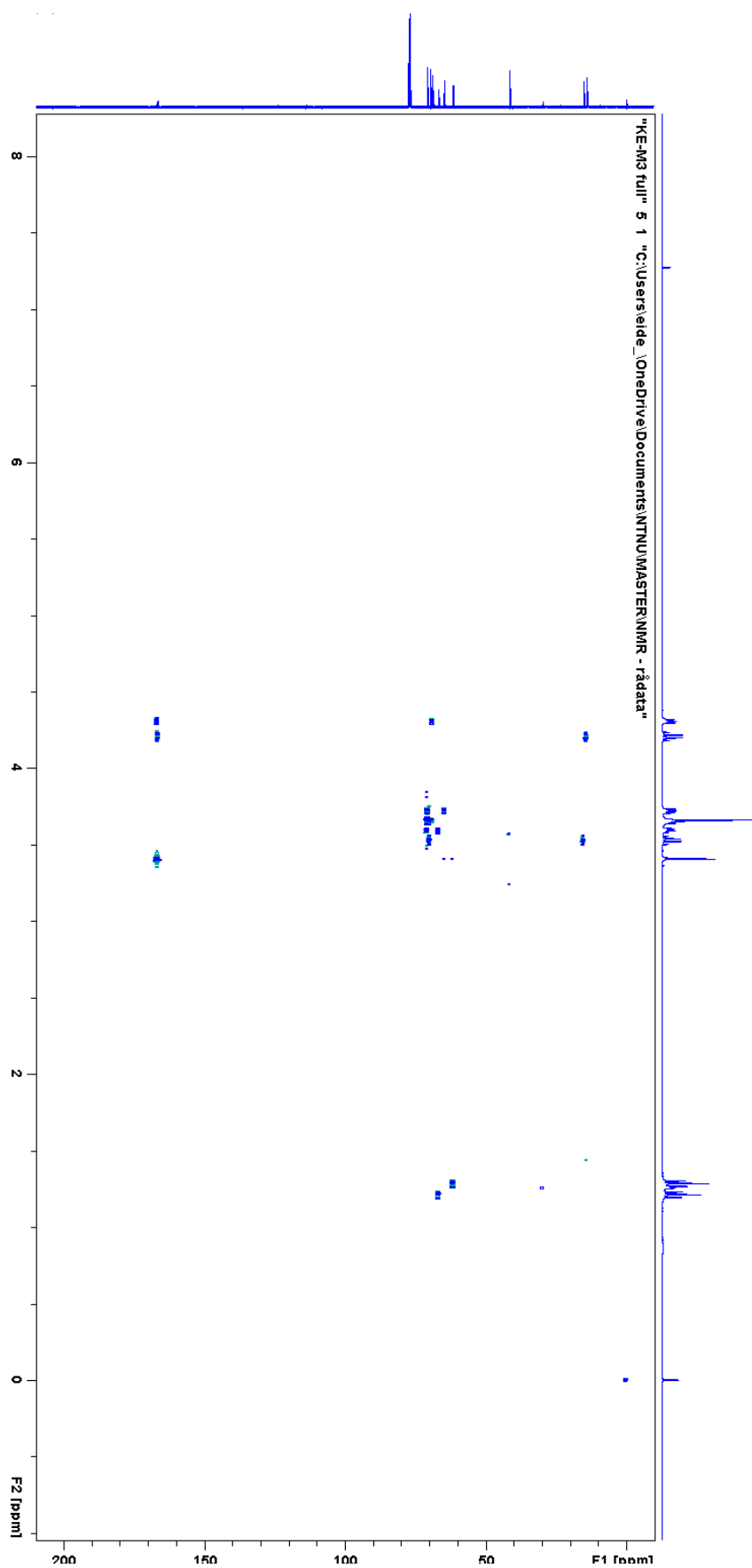


Figure 8.1.8: HMBC-spectra of KE-M3

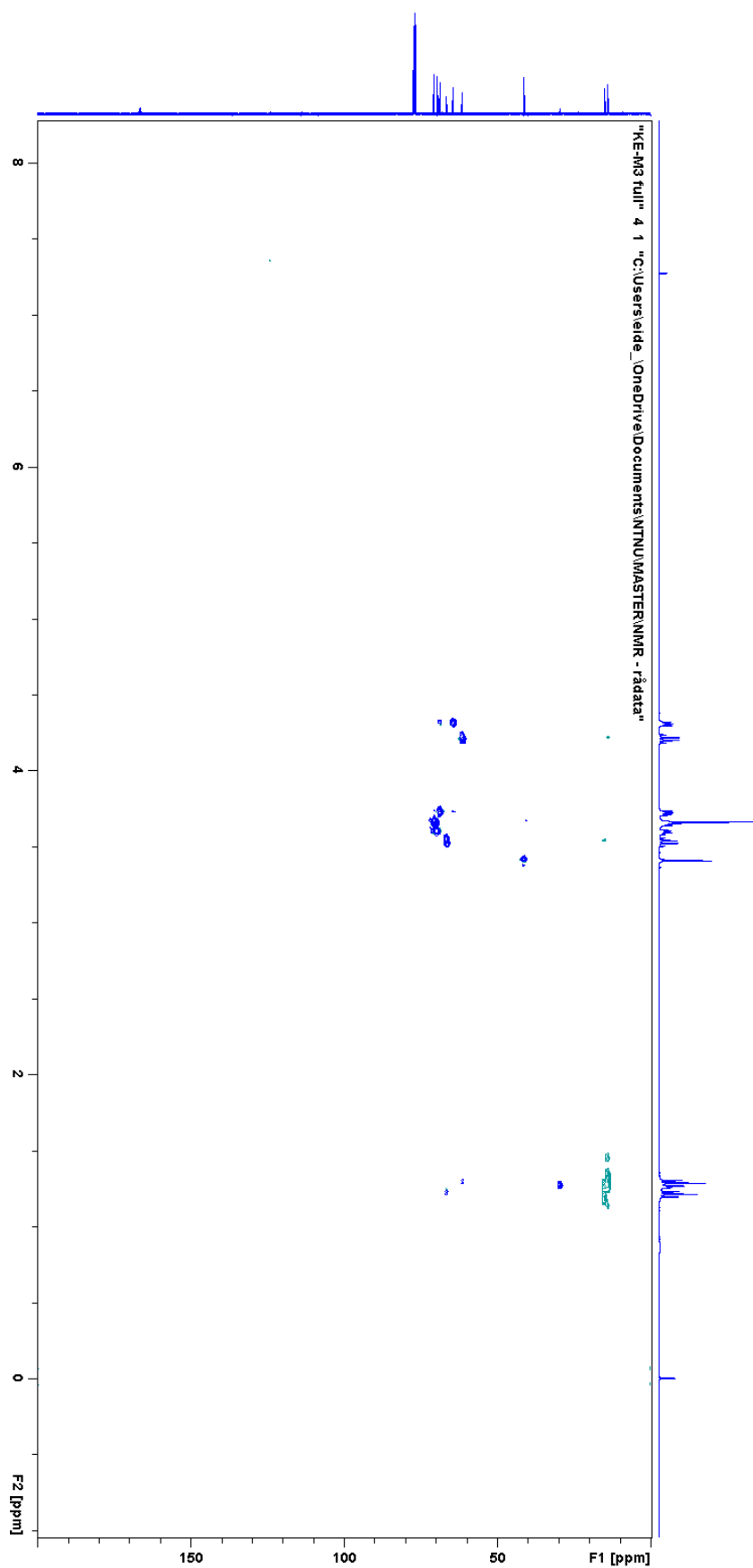


Figure 8.1.9: HSQC-spectra of KE-M3

8.2 MS of 2-(2-(2-ethoxyethoxy)ethoxy)ethylmalonate

Elemental Composition Report

Page 1

Single Mass Analysis

Tolerance = 2.0 PPM / DBE: min = -5.0, max = 50.0

Element prediction: Off

Number of isotope peaks used for i-FIT = 3

Monoisotopic Mass, Even Electron Ions

505 formula(e) evaluated with 2 results within limits (all results (up to 1000) for each mass)

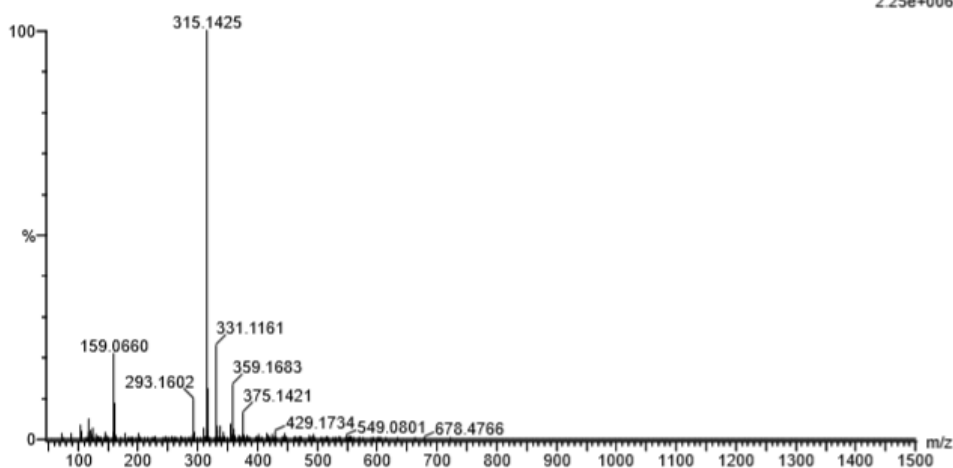
Elements Used:

C: 0-100 H: 0-100 N: 0-2 O: 0-10 Na: 0-1 Cl: 0-1

2020_168 48 (0.464) AM2 (Ar,35000.0,0.00,0.00); Cm (34:48)

1: TOF MS ES+

2.25e+006



Mass	Calc. Mass	mDa	PPM	DBE	i-FIT	Norm	Conf (%)	Formula
315.1425	315.1420	0.5	1.6	1.5	1328.8	0.000	100.00	C13 H24 O7 Na
	315.1422	0.3	1.0	-4.5	1350.7	21.913	0.00	C9 H28 O9 Cl

8.3 IR – spectra of 2-(2-(2-ethoxyethoxy)ethoxy)ethylmalonate

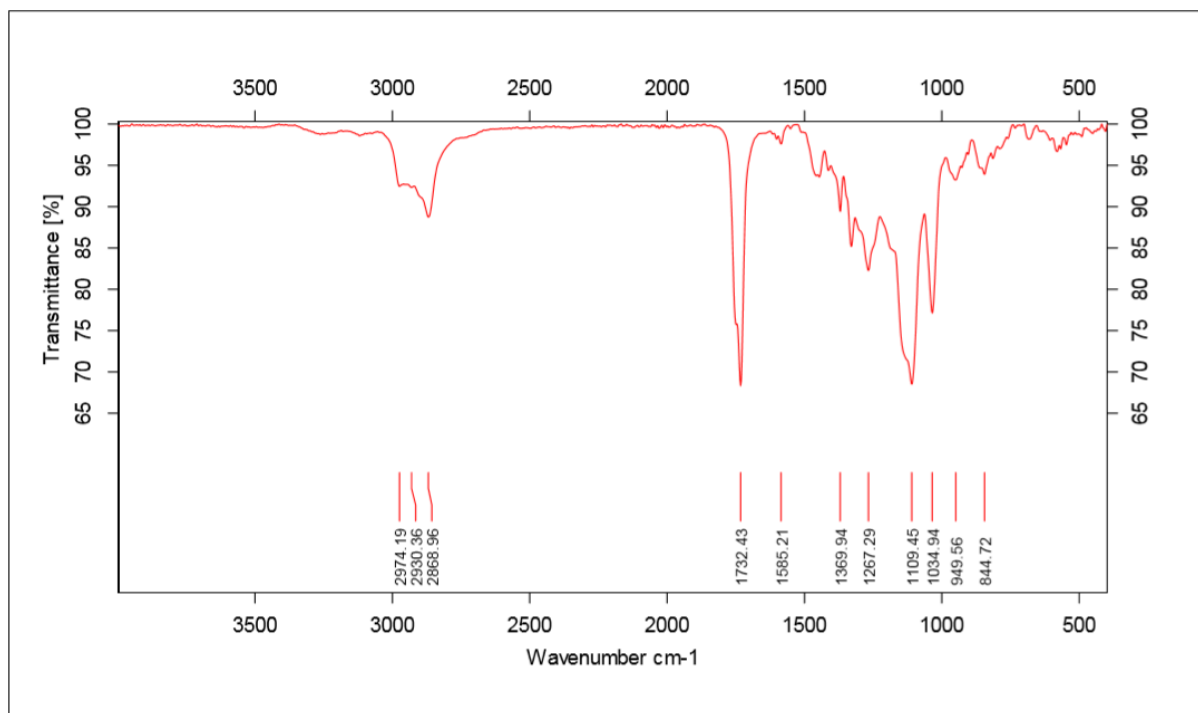



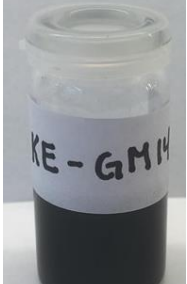

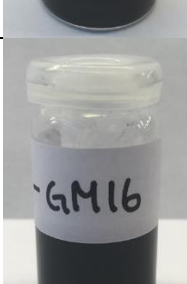

Figure 8.3.1: IR-spectra of 2-(2-(2-ethoxyethoxy)ethoxy)ethylmalonate

8.4 Preparation and functionalization of graphene

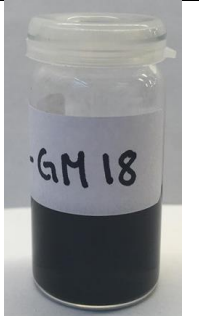
Table IX: Preparation and functionalization of graphene

Name	Graphene				CBr ₄ [g]	Malonate		DBU [mL]	Microwave				
	[Watt]	[mL]	cooling	[min]		Sample	[mL]		[°C]	Time	Wattage	Pressure	Cooling
FM-1	63	2,50	no	30	0,5740	KE-M1	0,50	0,40	130	20	50	5 bars	No
FM-2	-	3,65	-	-	0,5984	-	-	-	120	30	-	-	On
KE-GM1	-	2,50	yes	2*30	0,4140	KE-M2	-	-	-	25	40	-	No
NJ-GM1	-	-	-	-	0,5161	NJ	0,45	-	-	-	-	-	On
KE-GM2	-	-	-	-	0,4729	KE-M1	0,50	-	-	-	-	-	-
KE-GM3	-	2,00	-	-	0,4929	KE-M2	0,45	-	-	20	-	-	-
KE-GM4*	-	2,50	-	-	0,4611	-	0,40	-	-	30	-	-	-
KE-GM5*	-	2,30	-	-	0,4565	-	-	-	-	-	-	-	-
KE-GM6*	-	2,50	-	-	0,4974	-	0,43	-	-	-	-	-	-
KE-GM7	-	-	-	-	0,5103	NS-M1	0,40	-	-	-	-	-	-
KE-GM8	-	3,00	-	-	0,5549	-	0,45	-	-	-	-	-	-
KE-GM9	-	-	-	-	0,4221	-	0,40	-	-	-	-	-	-
KE-GM10	-	-	-	30	0,4921	KE-M3	0,30	-	-	25	-	-	-
KE-GM11	-	-	-	-	0,4244	KE-M3	0,35	-	-	-	-	-	-
KE-GM12	-	-	-	-	0,4946	KE-M3	0,30	-	-	-	-	-	-
KE-GM13	-	-	-	-	0,5640	-	0,10	-	-	-	-	-	-
KE-GM14*	-	-	-	-	0,5651	-	0,10	-	-	-	-	-	-
KE-GM15*	-	-	-	-	0,5405	-	0,05	-	-	-	-	-	-
KE-GM16	-	-	-	-	0,5055	-	0,05	-	-	-	-	-	-
KE-GM17	-	-	-	-	0,5086	-	0,025	-	-	-	-	-	-
KE-GM18*	-	-	-	-	0,5372	-	0,010	-	-	-	-	-	-
KE-GM19*	-	-	-	-	0,2459	-	-	-	-	-	-	-	-
KE-GM20*	-	-	-	-	0,1222	-	-	-	-	-	-	-	-
KE-GM21*	-	-	-	-	0,0685	-	-	0,05	-	20	-	-	-
KE-GM22*	-	-	-	-	0,0753	KE-M5	-	-	-	10	-	-	-
KE-GM23*	-	-	-	-	0,0514	-	-	-	-	-	-	-	-
KE-GM24*	-	-	-	-	0,0756	-	-	-	90	-	30	-	-
KE-GM25*	-	5,00	-	-	0,0671	-	-	-	120	-	40	-	-
KE-GM26*	-	3,00	-	-	0,0743	KE-M4	-	-	-	20	30	-	-
KE-GM27*	-	-	-	-	0,0607	-	-	-	-	10	40	no	-
KE-GM28*	-	-	-	-	0,0667	-	-	-	-	-	-	5 bars	no
KE-GM30*	-	9,00	-	-	0,2154	-	0,030	0,20	-	30	-	-	on

Table X: Different samples of functionalized graphene with different amount of malonate and with figure.

Sample	CBr ₄	Malonate	Graphene		DBU	Figure
	[g]	[mL]	mL	Solvent	[mL]	
KE-GM13	0.5640	0.1	3.0	σ -DCB	0.4	
KE-GM14	0.5651	0.1	3.0	NMP	0.4	
KE-GM15	0.5405	0.05	3.0	NMP	0.4	
KE-GM16	0.5055	0.05	3.0	σ -DCB	0.4	
KE-GM17	0.5086	0.025	3.0	σ -DCB	0.4	

Appendix

KE-GM18	0.5372	0.010	3.0	NMP	0.4	
---------	--------	-------	-----	-----	-----	---

8.5 IR – spectra of functionalized graphene

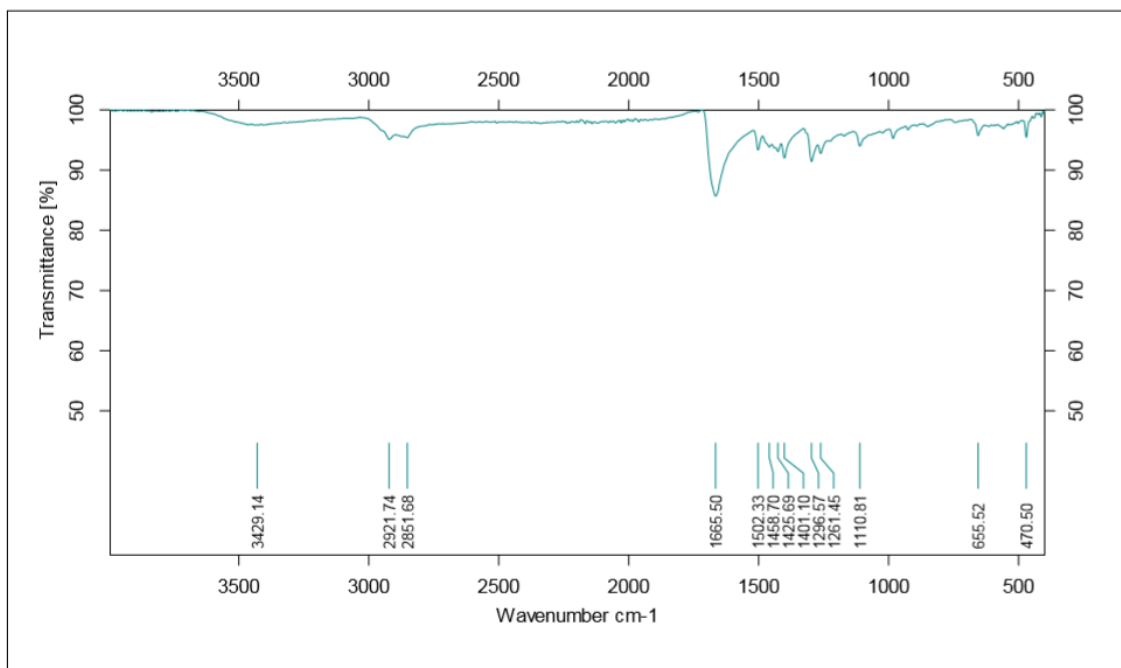


Figure 8.5.3: IR-spectra of sample KE-GM18.

